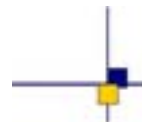


Validation of altimeter data by comparison with tide gauge measurements

for TOPEX/Poseidon, Jason-1, Jason-2 and Envisat

Contract No 104685/00 - lot1.2A



Reference : CLS.DOS/NT/13-285

Nomenclature : SALP-RP-MA-EA-22294-CLS

Issue : 1rev 1

Date : May 6, 2014



| Chronology Issues: | | |
|---------------------------|------------------|------------------------|
| Issue: | Date: | Reason for change: |
| 1.0 | 18 December 2013 | Creation |
| 1.1 | 06 May 2014 | Update of the document |
| | | |

| People involved in this issue: | | |
|---------------------------------------|---------------------------|-----|
| Written by: | P. Prandi G. Valladeau | CLS |
| Checked by: | S. d'Alessio | CLS |
| Approved by: | J.P. Dumont M. Ablain | CLS |
| Application authorized by: | | |

| Index Sheet: | |
|---------------------|--|
| Context: | |
| Keywords: | |
| Hyperlink: | |

| Distribution: | | |
|----------------------|-----------------------|----------------------------|
| Company | Means of distribution | Names |
| CLS/DOS | 1 electronic copy | G.DIBARBOURE |
| | 1 electronic copy | M.ABLAIN |
| DOC/CLS | 1 electronic copy | DOCUMENTATION |
| CNES | 1 electronic copy | thierry.guinle@cnes.fr |
| CNES | 1 electronic copy | aqgp_rs@cnes.fr |
| CNES | 1 electronic copy | dominique.chermain@cnes.fr |
| CNES | 1 electronic copy | delphine.vergnoux@cnes.fr |
| ESA | 1 electronic copy | P.FEMENIAS |

List of tables and figures

List of Tables

1 *Corrections applied for altimetric SSH calculation* 41

List of Figures

1 *Left: Location of the GLOSS/CLIVAR tide gauges. Right: Location of the PSMSL tide gauges.* 4

2 *Acquisition procedure of tide gauge data and conversion to "in-situ measurements tables" specific format.* 5

3 *general workflow of the altimetry versus tide gauges comparison process* 6

4 *schematic representation of the pre-processing of satellite altimetry data* 7

5 *schematic representation of the pre-processing of in-situ data* 8

6 *schematic representation of the process used to generate collocated satellite altimetry and in-situ time series* 9

7 *representation of the global averaging methodology* 11

8 *Monitoring of the number of tide gauges considered in the comparison between in-situ data and DUACS DT altimeter products* 12

9 *Cycle by cycle monitoring of mean SLA differences between T/P and tide gauge measurements. The red points represent the raw data while the blue curve is obtained after applying a two months running mean filter.* 13

10 *time series of global average differences between Jason-1 and tide gauges (10a) and between Jason-2 and tide gauges (10b). The red points represent the raw data while the blue curve is obtained after applying a two months running mean filter* 14

11 *seasonal cycle of the altimetry-tide gauges differences for Jason-1 (red) and Jason-2 (blue), and Topex/Poséidon (green) data* 15

12 *time series of global average differences between Jason-1 and tide gauges and between Jason-2 and tide gauges after removing the seasonal cycle. The red points represent the raw data while the blue curve is obtained after applying a two months running mean filter* 15

13 *time series of the global average differences between altimetry and tide gauges for Jason-1 and Jason-2 missions, restricted to the overlapping period between the missions* 16

14 *Temporal evolution of the number of tide gauges used in the estimation of global average differences between Jason-1 and in-situ records* 17

15 *time series of the global average differences between Envisat and tide gauges (15a) alone, and compared to Jason-1 (15b)* 17

16 *Temporal evolution of the number of tide gauges used in the estimation of global average differences between Envisat and in-situ records.* 18

17 *time series of global average differences between Duacs merged product (17a), Duacs mono-mission product (17b) and tide gauges data* 19

18 *Impact of the GPD wet tropospheric correction on SLA trends (in $mm.yr^{-1}$) estimated from TOPEX/Poseidon data* 20

19 *Histogram of altimetry minus tide gauge variance differences in the Indian Ocean* . . 21

.....

| | | |
|----|---|----|
| 20 | <i>Left: Trend of the SSH differences between Jason-1 and tide gauge measurements considering level-2 data or an objective analysis. Right: Monitoring of the standard deviation and number of tide gauges considered using Jason-1 along-track data (AT) or an objective analysis (AO)</i> | 22 |
| 21 | <i>Histogram of the standard deviation of trend differences considering Jason-2 level-2 data or an objective analysis</i> | 22 |
| 22 | <i>Time series of SSH differences between Jason-1 and the tide gauge at station Kushimoto</i> | 24 |
| 23 | <i>Two examples of the empirical fluctuation tests applied on the time series of figure 22</i> | 25 |
| 24 | <i>Example of a tide gauge information card</i> | 27 |
| 25 | <i>Numerical prediction of the rates induced by GIA on present day sea level change measured by tide gauges (top), satellite altimetry (middle) and by a gravity mission like GRACE (bottom).</i> | 29 |
| 26 | <i>GIA correction to be applied to satellite altimetry SSH rates derived from the ICE5G/VM2 model.</i> | 30 |
| 27 | <i>Time series of global average differences between altimetry and tide gauges using the current (red) and alternate (blue) methods for correcting GIA signals on altimetry data.</i> | 31 |
| 28 | <i>Histogram of trends of the differences between altimetry and tide gauge data, without any GIA correction (red), with tide gauges corrected for GIA (blue), and with tide gauges and altimetry corrected for GIA signals (green).</i> | 32 |
| 29 | <i>Number of GLOSS/CLIVAR tide gauges considered in the comparison with GeoSat between 1985 and 1990.</i> | 33 |
| 30 | <i>Left: Trend of SSH differences between GeoSat and tide gauges on the repetitive orbit (mm/yr). Right: Standard deviation (red curve) and number (blue curve) of the comparison between GeoSat's repetitive orbit data and GLOSS/CLIVAR tide gauge measurements.</i> | 34 |

List of items to be defined or to be confirmed

Applicable documents / reference documents

Contents

| | |
|--|-----------|
| 1. Introduction - Document overview | 1 |
| 2. Database: a review of tide gauges datasets in use | 3 |
| 2.1. Overview | 3 |
| 2.2. Tidal networks | 3 |
| 2.3. Acquisition and post-processing steps | 4 |
| 3. Methodology: a careful description of the altimeter/tide gauges comparison procedure | 6 |
| 3.1. Overview | 6 |
| 3.2. Pre-processing of altimetry and in-situ data | 7 |
| 3.2.1. Satellite altimetry data | 7 |
| 3.2.2. Tide gauge data | 8 |
| 3.2.2.1. High frequency signals | 8 |
| 3.2.2.2. Vertical motion of the tide gauge benchmark | 8 |
| 3.3. Station-wise comparison between altimetry and tide gauge data | 9 |
| 3.3.1. Temporal resampling | 9 |
| 3.3.2. Correlation estimation, quality check and extraction | 9 |
| 3.3.3. Referencing of tide gauges time series | 10 |
| 3.4. Computation of global statistics | 10 |
| 3.5. Summary | 11 |
| 4. Detection of drifts and jumps on global altimeter records | 12 |
| 4.1. Analysis on TOPEX/Poseidon | 12 |
| 4.2. Analysis on Jason-1 and Jason-2 altimeter missions | 13 |
| 4.3. Analysis on Envisat mission | 17 |
| 4.4. Analysis on multi-mission gridded datasets | 18 |
| 4.4.1. SSALTO/DUACS maps of Sea Level Anomaly | 18 |
| 4.4.2. ESA's Sea Level Climate Change Initiative dataset | 19 |
| 5. Evaluation of new altimeter standards or methods | 20 |
| 5.1. Overview | 20 |
| 5.2. Evaluation of the GPD wet tropospheric correction | 20 |
| 5.3. Impact of the objective analysis on altimeter/tide gauges comparisons | 21 |
| 6. Quality assessment of tide gauge time series | 23 |
| 6.1. Detection of structural changes in in-situ time series | 23 |
| 6.1.1. Position of the problem | 23 |
| 6.1.2. Methodology | 23 |
| 6.1.3. Results | 24 |
| 6.1.4. Conclusions and Futures | 25 |
| 6.2. A new design for in-situ information cards | 25 |
| 6.2.1. Description of the information cards | 25 |
| 7. 2013 Particular Investigations | 28 |
| 7.1. Accounting for GIA effects on altimetry data | 28 |
| 7.1.1. Theoretical elements | 28 |
| 7.1.2. Current strategy | 29 |

| | |
|---|-----------|
| 7.1.3. Alternate strategy | 30 |
| 7.1.4. Experiment | 30 |
| 7.1.5. Results | 31 |
| 7.1.6. Conclusions | 32 |
| 7.2. Comparing the new GeoSat dataset with tide gauge measurements | 32 |
| 7.2.1. Results | 33 |
| 7.2.2. Conclusion | 34 |
| 8. Conclusions | 35 |
| 9. References | 38 |
| 10. Annexes | 40 |
| 10.1. Annex: Corrections applied for altimeter SSH calculation | 40 |
| 10.2. Annex: Evaluation of the Sea Level CCI dataset with respect to in-situ data | 42 |
| 10.3. Annex: New design of simplified in-situ information cards | 67 |
| 10.4. Annex: Global quality assessment of updated GeoSat dataset | 69 |

1. Introduction - Document overview

This document is the altimeter/tide gauges comparison activities synthesis report for 2013, performed in the frame of the 2011-2015 SALP project (CNES) and supported by ESA concerning Envisat.

Calibration and validation of altimeter data is widely processed by comparison with in-situ time series since they provide external and independent information to be used as a reference (note that a synthesis report on the cross-comparison between altimeter data and Argo T/S profiles is also available). Indeed, tide gauge measurements and Argo T/S profiles constitute two complementary datasets for this activity. Although the spatial coverage is worse with tide gauges (only a few part of coastal areas are covered while the Argo network can sample the global open ocean), the temporal sampling of tide gauge measurements is really better (one measure each hour whereas one profile every ten days for Argo T/S profiles). That be, the combination of the several results obtained through this activity can be considered as reliable thanks to the use of multiple in-situ datasets. Moreover, these cross-comparisons with external independent in-situ measurements increase the quality of calibration and validation of altimeter measurements.

Whatever in-situ dataset used in the frame of this activity, tide gauge measurements as well as Argo T/S profiles, these studies are focusing on the comparison with the Sea Surface Height (SSH) derived from altimetry in order to:

1. Detect drifts and jumps in the altimeter sea level time series and give an assessment of the global and regional MSL trend
2. Estimate the potential improvement provided by new altimeter standards (orbit solution, geophysical corrections...) on the SSH consistency
3. Perform a quality control of the in-situ time series, where drifts and jumps can remain, with no physical signification (drift of sensors, anthropogenic sources ...)

This complementary approach tends to improve our knowledge of the measured physical content, where tide gauges provide high temporal resolution of SSH in coastal regions whereas T/S profiles of the Argo network provide sea level dynamic heights in the almost whole global open ocean with a 10-day sampling.

In the first place, the document describes the tide gauge database used and its computation in order to make it comparable to the altimeter SSH. The tide gauge networks used and the data availability are further detailed, and new corrections used in the in-situ SSH calculation are also specified. The different step of the methodology used to compare altimetry data to tide gauges is also precisely described.

Concerning this activity, some new improvements were performed in 2013, about the tide gauge database but also on the accuracy of the results computed from the processing sequence. A new acquisition process of tide gauge measurements is routinely processed and includes the large PSMSL

tide gauge database, which latter will be soon considered in our comparisons. We developed new statistical tools to assess the quality of tide gauge time series, that will be useful to increase the reliability of global altimeter drifts estimate.

In addition to the particular investigations performed in 2013 and partially discussed above, the document describes the main results concerning the detection of the altimeter MSL drift for TOPEX/Poseidon (T/P), Jason-1, Jason-2 and Envisat.

The comparison procedure of new altimeter standards is also presented and discussed from temporal and spatial diagnoses, especially through the variance differences of both reference and studied parameters.

Finally, the report tackles the cross-comparison indicator performed on tide gauges to highlight spurious measurements and the futures of this activity, especially on the 2014 scientific investigations to be performed.

2. Database: a review of tide gauges datasets in use

2.1. Overview

The tidal database consists in records of tide gauges Sea Surface Height (SSH) from independent networks. Several types of geophysical corrections such as tide, pressure and wind effects are then applied on these raw data so as to deduce filtered Sea Level Anomalies (SLA) from tide gauge sea surface height in order to be consistent with altimeter data. The comparison of the latter with tide gauge measurements is thus made possible thanks to this tidal database and softwares dedicated to its computation. This section details the way of manipulating tide gauge measurements.

A new way to acquire tide gauge data was presented last year. This work on the improvement on the database, which is very important for reliable comparisons with altimetry, has been carried on this year in order to provide an operational solution to tide gauge end users.

Two different database are from now on available. The first one is the download and the storage of the raw data in CLS format, with the whole information about each tide gauge (name, network, coordinates, quality and other miscellaneous information). The second one(s) is(are) the database(s) dedicated to the comparison with altimetry, updated with different standards (oceanic tide, land motion, ...) in order to get fully post-processed tide gauge measurements. Multiple post-processed databases can be set up, depending on the temporal resolution of the tide gauge time series. Note that although the first step of this acquisition is the same for all networks (easy download data from ftp, http addresses or even process local data), the post-processing is specific for each one.

2.2. Tidal networks

The historical tidal database consisted in different tide gauges networks resulting from different collaborations. The data covered several time periods and were used for many kind of scientific studies. With the same goal, the new database has been supplied with two global tidal networks, weekly updated and post-processed:

- GLOSS/CLIVAR (Global Sea Level Observing System/Climate Variability and Predictability): time series of about 250 tide gauges are acquired with a temporal resolution of one hour. These measurements are used for tide prediction as well as altimetry validation.
- PSMSL (Permanent Service for Mean Sea Level): almost 1350 tide gauges of this network are computed in the tidal database (www.psmsl.org/), with a temporal resolution of 30 days. Data of these tide gauges are homogeneously computed and are relevant for climate studies.

Note that both datasets provide a global sampling for reliable studies about long-term sea level variability, globally and regionally (figure 1).

Finally, concerning the Senetosa tide gauge, time series of the M3, M4, M5 and M7 sensors are available on the AVISO website (www.aviso.oceanobs.com), where the in-situ section is divided into 2 parts, one concerning the absolute calibration and the other dedicated to the global comparison

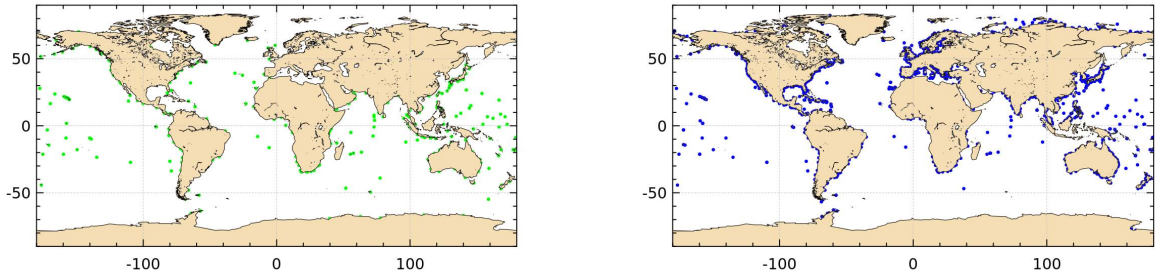


Figure 1: Left: Location of the GLOSS/CLIVAR tide gauges. Right: Location of the PSMSL tide gauges.

with altimetry.

2.3. Acquisition and post-processing steps

For the whole tidal networks, tide gauge measurements are computed and archived according to a linear procedure:

- 1. Weekly download of the updated data
- 2. Conversion from the original-sized data to the CLS-sized data (in-situ measurements tables) with several steps of validation
- 3. Implementation of dedicated filters for tide gauge data in order to remove the short and long tide wavelengths (diurnal, semi-diurnal and long period tides)
- 4. Record of the high resolution dynamical atmospheric correction (MOG2D model) to remove high frequency signals

As said previously, two different database have been processed in 2013 and consist of two parts. First the acquisition procedure, supplied with the raw sea surface height and the several static information (name, network, coordinates, ...). Then, the post-processing of the raw data and the dedicated corrections used to calculate an altimeter-coherent SSH.

The global procedure of the database for the acquisition process is presented in figure 2. By the means of "in-situ measurements tables" specific format, SSH measured by tide gauges can be filtered from high frequency phenomena quoted above. To date, the tidal database is considered as an operational system and updated every week according to the availability of new tide gauge measurements.

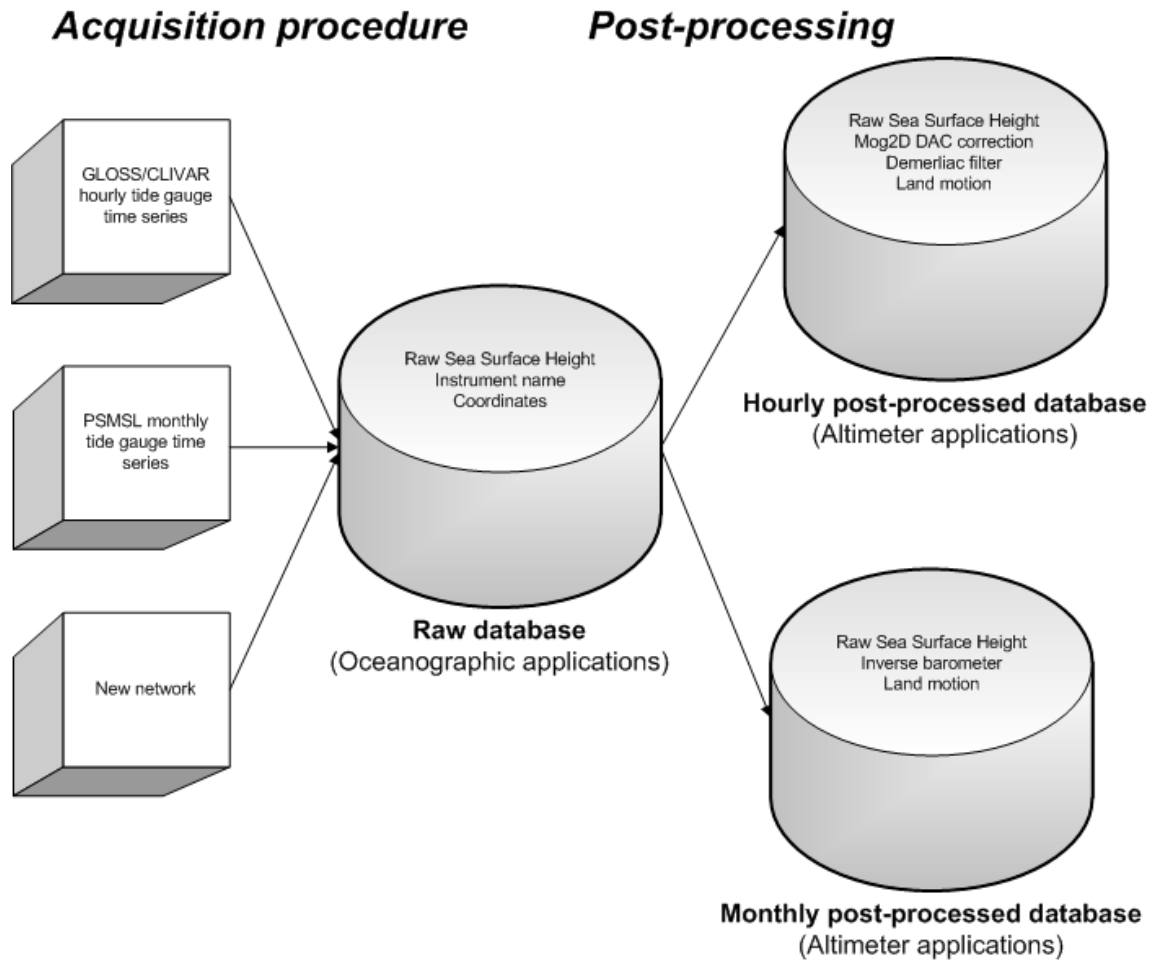


Figure 2: Acquisition procedure of tide gauge data and conversion to "in-situ measurements tables" specific format.

3. Methodology: a careful description of the altimeter/tide gauges comparison procedure

3.1. Overview

In the present section of this report, we provide a careful description of the processing used at CLS to compare altimetry data to in-situ measurements from tide gauges. Different schematic representations of the processing are used to ease the description. We used a consistent representation rule to display the different elements of the processing:

- processing steps that imply a transformation of the input data are displayed as rectangles,
- processing steps that do not transform the input data are displayed as diamonds,
- the original databases are displayed as tube sections (rectangles with curved vertical sides),
- intermediate datasets are displayed as parallelograms.

Figure 3 displays a schematic overview of the processing:

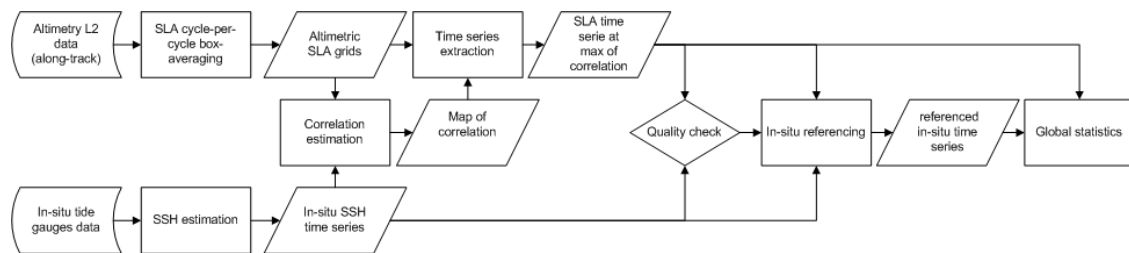


Figure 3: general workflow of the altimetry versus tide gauges comparison process

The major steps of this processing are:

- the pre-processing of altimetry and tide gauge data to derive sea level anomalies,
- the estimation of correlation maps between altimetry and tide gauge,
- the extraction of a satellite altimetry time serie for each tide gauge station,
- the referencing of the tide gauges time series with respect to altimetry data,
- the estimation of global statistics.

The five steps of the processing listed above are described with more details in the sections of the present chapter.

3.2. Pre-processing of altimetry and in-situ data

3.2.1. Satellite altimetry data

Radar altimeters provide Sea Surface Heights (SSH), which need to be referenced and corrected from geophysical signals to provide Sea Level Anomalies (SLA) comparable with in-situ measurements. When comparing to in-situ measurements from tide gauges, we use along-track (level 2) SSH from several satellite altimeters, where standards can be updated compared with the Geophysical Data Record (GDR) altimeter products. The Sea Level Anomalies (SLA) are computed from the along-track data according to equation 1:

$$SSH = Orbit - Altimeter\ Range - \sum_{i=1}^n Correction_i - Mean\ Sea\ Surface \quad (1)$$

where the corrections applied are:

$$\begin{aligned} \sum_{i=1}^n Correction_i = & \text{Dry troposphere correction} \\ & + \text{Dynamic atmospheric correction} \\ & + \text{Wet troposphere correction} \\ & + \text{Ionospheric correction} \\ & + \text{Sea state bias correction} \\ & + \text{Ocean tide} \\ & + \text{Solid earth tide} \\ & + \text{Geocentric pole tide} \end{aligned}$$

More details about the actual corrections used in SLA estimation (for example the model used to estimate the ocean tide) for each altimeter are can be found in annex 10.1.. In practice, the geophysical corrections usde follow the one used to estimate the global mean sea level. We use valid-only satellite altimetry measurements, and rely on a Cal/Val flag to perform this selection.

Along-track SLA are then averaged on a regular 2° by 2° grid, with a temporal sampling corresponding to each mission's repetitivity. This represents a change regarding last year's processing where 1° latitude by 3 ° longitude boxes were used for the averaging af satellite altimetry data.

The pre-processing applied to level 2 satellite altimetry data is summarized on figure 4.

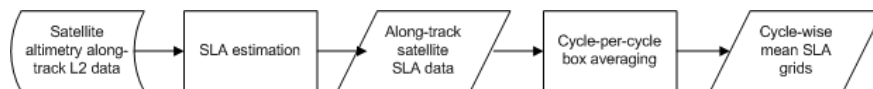


Figure 4: schematic representation of the pre-processing of satellite altimetry data

3.2.2. Tide gauge data

The goal of this pre-processing is to extract a corrected sea surface height time serie at each tide gauge station, with a physical content comparable to the satellite altimetry one. The relative sea surface height measured by tide gauges is different from the one from satellite altimeters, therefore the pre-processing to be applied to in-situ measurements differs from the satellite altimetry one.

The first difference is that tide gauges were designed to estimate tides, and, as a consequence generally have a much higher sampling rate than satellite altimetry records. Typically, tide gauges would sample the ocean every hour while, at a given point, the satellite altimetry sampling is higher than ten days. The second difference results from the fact that tide gauges measure the sea surface height relative to an on-ground benchmark. Every movement of this local datum has a direct effect on sea level measurements.

The pre-processing applied to in-situ measurements from tide gauges is summarized on figure 5.

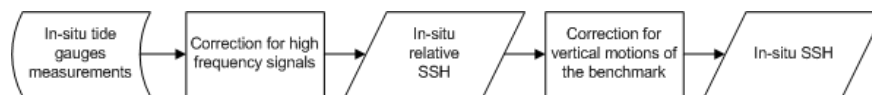


Figure 5: schematic representation of the pre-processing of in-situ data

3.2.2.1. High frequency signals

High frequency tidal effects on tide gauges data are corrected using the Dermerliac low-pass filter ([5, Bessero, 1985]). Long period tidal waves are also corrected using a specific algorithm based on well-balanced tide tables ([9, Cartwright and Eden, 1973]). High frequency atmospheric effects are corrected by withdrawing the Mog2d Dynamical Atmospheric Correction (DAC) (Dorandeu and Le Traon, 1999 [10]; Carrere and Lyard, 2003 [8]). Note that the correction applied also contains the inverse barometer effect.

Note that concerning PSMSL monthly data, the computation is slightly different: we do not correct the data for tidal and atmospheric high frequency effects. We consider these high frequency variations are filtered out when monthly averages of the data are computed (at PSMSL level). Therefore, we only apply on these data an ERA-interim derived inverse barometer correction.

3.2.2.2. Vertical motion of the tide gauge benchmark

One large uncertainty concerning tide gauge data is the vertical stability of the tide gauge benchmark over time. Vertical motions of tide gauges benchmarks can be monitored accurately using geodetic techniques such as DORIS or GPS levelling. In fact, only few stations are associated with such monitoring devices. As a consequence, we are not able to correct tide gauges for vertical motions of the benchmark derived from GPS or DORIS data.

One part of crustal motions is the response of the Earth's crust to the last deglaciation (known as GIA), which can induce large vertical motions. Models are available to estimate this effect, and predict vertical land motion rates over the globe. We use the ICE-5G/VM4 model [13, (Peltier, 2004)] to correct tide gauges time series for vertical land motion due to GIA.

3.3. Station-wise comparison between altimetry and tide gauge data

At this point of the processing workflow, both altimeter and tide gauge data show comparable SSH physical contents. The next step of the comparison process is to extract one satellite altimetry time serie at each tide gauge site. The process used to extract the altimetry time serie and to generate collocated time series at each tide gauge station is schematically described on figure 6. This processing is applied for each tide gauge station in the database. The different steps are described in the present section.

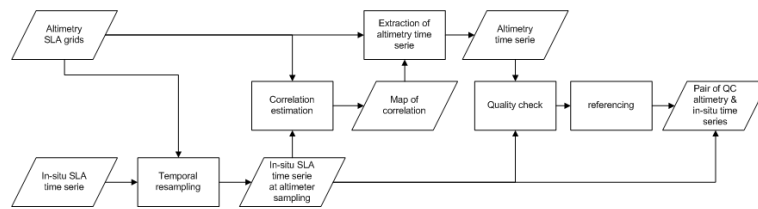


Figure 6: schematic representation of the process used to generate collocated satellite altimetry and in-situ time series

3.3.1. Temporal resampling

The temporal sampling of satellite altimetry corresponds to the repetitivity of the mission, while tide gauge measurements generally have a much higher temporal sampling frequency. Before performing any comparison between the two measurements, the high frequency tide gauge data are resampled at the low frequency of the altimetry data by performing an average over one altimeter cycle windows.

3.3.2. Correlation estimation, quality check and extraction

After resampling the tide gauge time series, a map of the correlation coefficients between the altimetry grids and the in-situ record is computed. Note that the tide gauge time serie has to contain at least 2 years of measurements to be taken into account.

The satellite altimetry time series is then extracted where the maximum of correlation is found, given that this maximum is found within a 150 km radius distance of the tide gauge, and that the satellite altimetry time serie matches a number of quality criteria. A satellite altimeter time serie is extracted if:

- the correlation between altimetry and tide gauge time series is higher than 0.7,
- the length of the satellite altimetry time serie is at least 80% of the corresponding tide gauge time serie over the common time span (too gappy altimeter records are rejected),
- the standard deviation of the differences between altimetry and tide gauge data does not exceed 10cm,
- the difference between altimetry and tide gauge data does not exceed 12cm (estimated after both time series are centered).

If one criteria is not fulfilled, the satellite altimeter time serie extracted at the next lower correlation value is tested, and so on iteratively. At the end of this step, for each tide gauge station, we have a matching satellite altimetry time serie, at the same temporal sampling and with similar physical contents.

3.3.3. Referencing of tide gauges time series

An important step of the processing is to reference tide gauge time series onto altimetry ones. Tide gauge measurements are referenced with respect to a local benchmark, whose position is generally given within the frame of a national datum system. In this processing, satellite altimetry is considered as a model for in-situ data to be referenced into a common frame. Therefore, the mean of the altimetry-TG SSH differences is computed and subtracted from each tide gauge time serie.

Using satellite altimetry to reference tide gauge time series implies an important limitation of all further analysis: this technique will prevent tide gauge measurements from detecting regional biases in altimeter records. This remains an important issue with our current comparison method. Investigating new referencing procedures and evaluating the sensitivity of the results should be a priority for next year's work.

3.4. Computation of global statistics

One of the main goals of the comparison procedure is to generate global statistics between altimetry and in-situ measurements, indicating the global drift of the level-2 satellite altimeter data.

At this moment, a set of pairs of collocated altimetry and in-situ time series that all meet the different quality criteria has been produced. The aim of this last step of the processing is to generate one global time serie of the differences between altimetry and in-situ from the larger set of collocated time series. This is performed by averaging all records together.

Tide gauges stations are unevenly distributed along the global coastline, and some regions (like the European Atlantic coasts) are oversampled while other areas (such as the southern ocean) are almost not observed. In order to mitigate the effects of this uneven sampling, the global mean average is estimated through a two step process:

- data are averaged first by 3° wide longitude bands,
- longitude bands are then averaged into the global mean.

The averaging method used to compute global mean averages from a set of collocated altimetry and tide gauges time series is schematically displayed on figure 7.

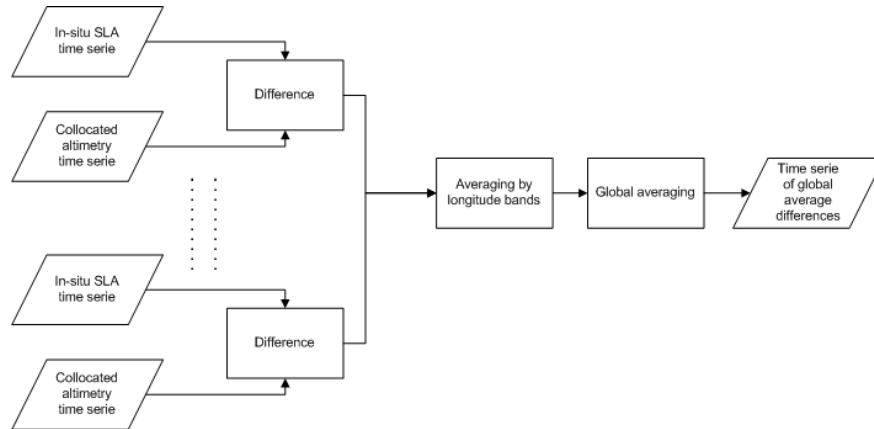


Figure 7: representation of the global averaging methodology

3.5. Summary

In the present section, we described the processing used to compare satellite altimetry data to in-situ sea surface height measurements from tide gauges. The result of this complex processing is to detect drifts or regime changes in satellite altimetry records by averaging the differences with in-situ time series.

4. Detection of drifts and jumps on global altimeter records

The cycle by cycle monitoring of global average differences between altimetry and in-situ sea surface height measurements provides a way to assess the satellite data quality and to detect jumps and drifts affecting sea level records.

In the present study, tide gauges from the GLOSS/CLIVAR database are compared to level-2 altimeter records. However due to the quality criteria that are applied, the average number of stations retained in each point of comparison may vary. The number of tide gauges considered differs from one altimetry mission to another, and over time for a given mission, depending on the availability/unavailability of the in-situ sensors. A typical evolution of the number of tide gauges used in the global average estimation is represented on figure 8. While an almost linear growth of the number of tide gauges, corresponding to the availability of new stations in the dataset, is displayed for the most part of the time period, a slight decrease can be observed at the end due to the time lag of the update of tide gauge measurements in the database.

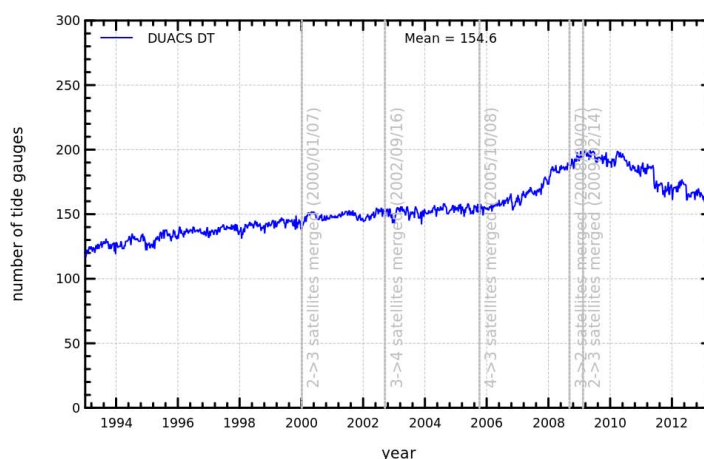


Figure 8: Monitoring of the number of tide gauges considered in the comparison between in-situ data and DUACS DT altimeter products

Moreover, note that all the time series presented in this section have been corrected for GIA effects on satellite altimetry data using a uniform -0.3 mm.yr^{-1} trend correction. Further details about this correction are available in section 7.1..

4.1. Analysis on TOPEX/Poseidon

Since T/P space mission delivered one of the longest available altimeter time series, the comparison with tide gauges has become of reference regarding studies about MSL drift. Results on the differences between T/P data and tide gauge measurements (figure 9) display a global trend of about 0.6 mm/yr over the 1993-2005 time period. Differences with previous results have been explained last

year with the change of the spatial resolution of the gridded altimeter SSH computed, especially on the TOPEX new orbit time period (2002-2005). Indeed the $1^\circ \times 3^\circ$ spatial sampling had an impact on the computation of the maximum of correlation on the whole time series. Applying the new $1^\circ \times 1^\circ$ altimeter gridded SSH solved this artefact. Furthermore, the low rms differences and the low formal adjustment error (< 0.1 mm/yr) is in favor of a reliable assessment of T/P global MSL on the whole altimeter time period. However, focusing on both TOPEX-A (cycles 11 to 236) and TOPEX-B (cycles 237 to 364) time periods, the behavior of the altimeter is quite different. Next to the improvements on the method, a better reliability on the consistency between altimeter data and tide gauge measurements is expected although the global trend slightly increased (around 0.6 mm/yr). However, some remaining drifts and high amplitude residual signals are still to be understood, especially over the TOPEX-A time period where a negative slope was highlighted between 1993 and 1996 and a positive one from 1996 to 1999. Although both TOPEX-A periods are likely too short (3 years) to determine an accurate drift by comparison with tide gauges, the TOPEX-B MSL appears more stable with no drift from February 1999 onwards. The significant positive drift detected on TOPEX-A from 1996 onwards corresponds to the beginning of the TOPEX-A anomaly (cycles 130 to 236) where strong instrumental instabilities have been highlighted on significant wave height and backscatter coefficient parameters (Ablain et al., 2012 [1]). Comparisons with tide gauges tend to demonstrate that these anomalies have also an impact on the sea-level stability during this period. On the beginning of TOPEX-A from 1993 to 1996, thorough investigations have to be performed to explain the negative drift observed. Although T/P provides accurate measurements for climate studies, the long-term stability of TOPEX-A data could be improved.

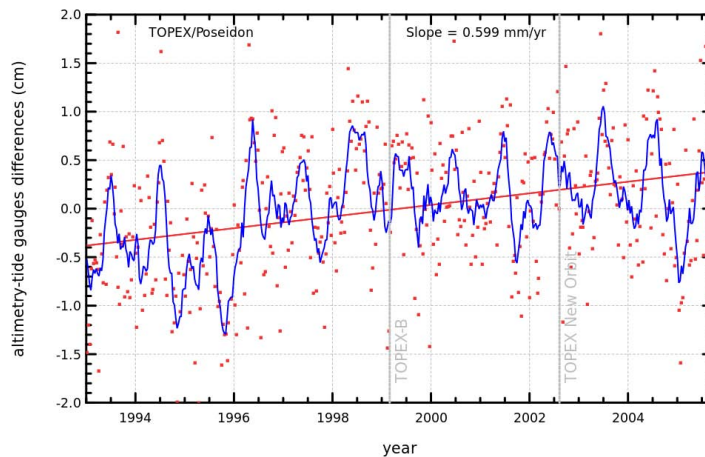


Figure 9: Cycle by cycle monitoring of mean SLA differences between T/P and tide gauge measurements. The red points represent the raw data while the blue curve is obtained after applying a two months running mean filter.

4.2. Analysis on Jason-1 and Jason-2 altimeter missions

Figure 10 displays the time series of global average differences between Jason-1 (left), Jason-2 (right) and tide gauges. Considering both altimeter missions, the comparison with tide gauges measurements provides consistent long-term trend differences (0.2 mm/year for Jason-1, 0.1 mm/year for

Jason-2), with a low formal adjustment error, close to 0.1 mm/yr. The coherence with in-situ measurements along coastal areas is pretty good, and rms differences are lower than 4 cm.

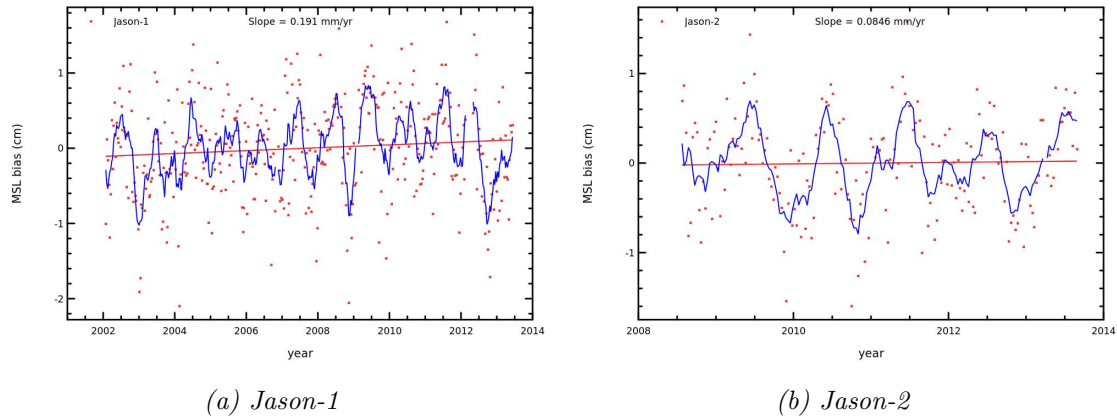


Figure 10: time series of global average differences between Jason-1 and tide gauges (10a) and between Jason-2 and tide gauges (10b). The red points represent the raw data while the blue curve is obtained after applying a two months running mean filter

Looking further at these monitoring, one of the first thing that stands out is the significant annual cycle in the time series of the differences. This annual cycle is emphasized on figure 11 which represents the seasonal cycle extracted from the time series plotted on figure 10 and figure 9. For all three missions, a similar seasonal cycle is observed on the differences between altimetry and in-situ. Its amplitude is about one centimeter (a bit higher for Jason-2 than for Jason-1 and Topex). All seasonal cycles have similar shapes, the maximum is reached in May while it bottoms the minimum in October (Jason-2), November (Jason-1) or September (Topex).

The origin of such annual signal in the time series of the differences is still unknown, it may originate from different sources, for example:

- a true difference between annual cycles at the coast (as measured by tide gauges) and offshore (as seen by altimetry data),
- a potential pollution of the global average by a few tide gauges located up in river estuaries and thus influenced by river discharge,
- an annual cycle in vertical land motion not corrected for in tide gauges data,
- or one of the geophysical corrections.

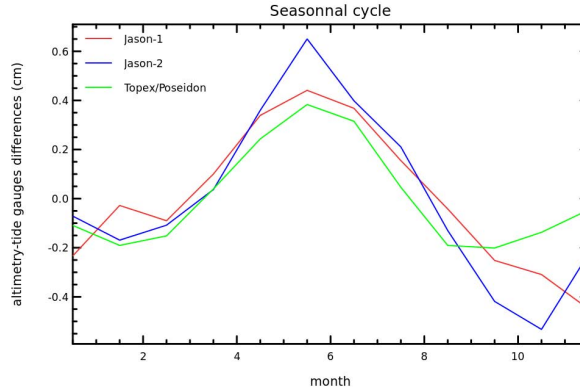


Figure 11: seasonal cycle of the altimetry-tide gauges differences for Jason-1 (red) and Jason-2 (blue), and Topex/Poséïdon (green) data

Once the annual signal is removed, one can reliably estimate the long term trend of the global average differences time series. Figure 12 thus displays the global average differences between collocated satellite altimetry and tide gauges SSH records, with the annual signal removed. For the Jason-1 mission, the long term trend amounts to 0.2 mm.yr^{-1} while it is close to -0.2 mm.yr^{-1} for the Jason-2 mission. Given the trend values observed, we see no significant drifts between either Jason-1 or Jason-2 and in-situ SSH measurements from tide gauges. Moreover, the standard deviation of the filtered time series are in agreement between both altimeter missions, respectively 0.3 and 0.2 cm for Jason-1 and Jason-2.

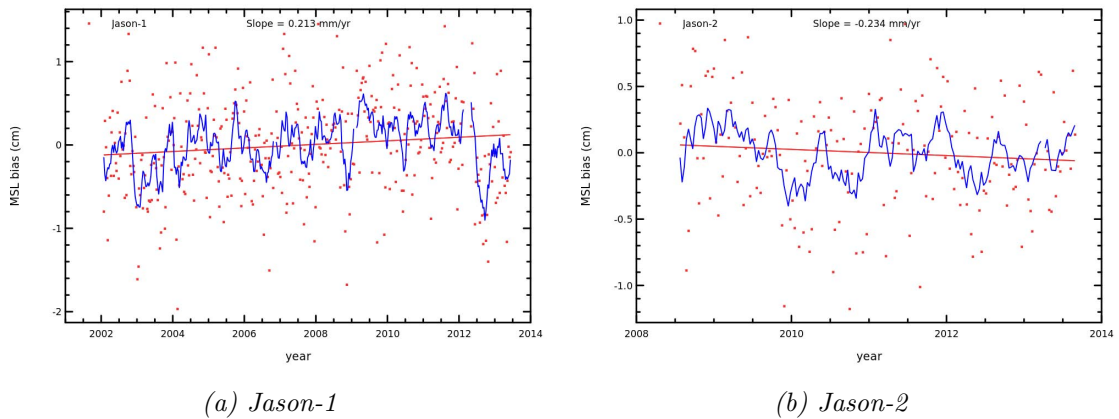


Figure 12: time series of global average differences between Jason-1 and tide gauges and between Jason-2 and tide gauges after removing the seasonal cycle. The red points represent the raw data while the blue curve is obtained after applying a two months running mean filter

Furthermore, on the overlapping period of Jason-1 and Jason-2, both missions show global mean sea level (GMSL) trends that differ by about 0.8 mm.yr^{-1} (see 2013 Jason-2 annual report [4]). The GMSL trend difference is reduced when using the model derived wet tropospheric correction rather than the radiometer one. The results of the comparison to tide gauges of both missions restricted to overlapping period are presented on figure 13. Figure 13a is obtained using the radiometer wet tropospheric correction, and the observed differences in global average differences between altimetry and in-situ data amounts to $\approx 0.6 \text{ mm.yr}^{-1}$ without annual and semi-annual signals, a value which is consistent with the observed discrepancy on GMSL trends. Switching to the model

wet tropospheric correction leads to the time series of figure 13b. The trend difference is reduced to about 0.3 mm.yr^{-1} , mainly due to an impact on Jason-2 data, but still consistent with the observed GMSL trends.

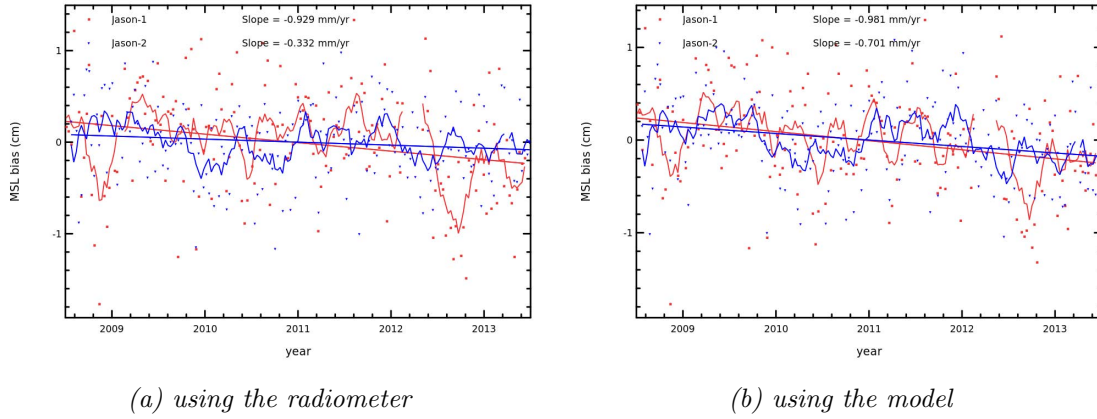


Figure 13: time series of the global average differences between altimetry and tide gauges for Jason-1 and Jason-2 missions, restricted to the overlapping period between the missions

Finally, the number of tide gauges considered on the whole Jason-1 time period has been further studied. Indeed, during its geodetic phase the comparison to tide gauges seems to indicate a bias of this mission phase with respect to in-situ measurements. When separating the two phases of the mission, the mean values differ by 0.3 cm. This appears to be statistically significant given a rough evaluation of the uncertainty on the estimator of the mean over the two phases based on a classical formulation for the uncertainty $U = t_{\%} \frac{\sigma}{\sqrt{N}}$, where $t_{\%}$ is a given percentile of Student's law.

The bias to link data from the geodetic phase of Jason-1 to the previous repetitive phase was evaluated globally, and maybe a geographically correlated pattern might impact the comparison to tide gauges. However it should be noted that the change of the ground track might impact the comparison methodology. Figure 14 displays the number of tide gauge stations used to estimate the global average difference over time and shows a strong drop at the beginning of the geodetic phase of the mission. When the geodetic phase of Jason-1 is not considered in the comparisons, the trend of the global average differences between altimetry and in-situ amounts to 0.5 mm.yr^{-1} . This value is still below the estimated uncertainty of the comparison method. However, some further investigations will be performed on the comparison procedure to better take both phases into account in the computation of the global trend of SSH differences.

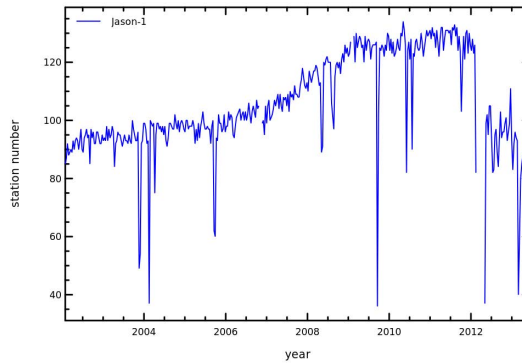


Figure 14: Temporal evolution of the number of tide gauges used in the estimation of global average differences between Jason-1 and in-situ records

4.3. Analysis on Envisat mission

As for Jason-1 and Jason-2, Envisat measurements are computed in order to provide an accurate assessment of the SSH. The trend of the altimeter minus tide gauges SSH differences amounts to 0.8 mm.yr^{-1} (see figure 15a), which is higher than the estimated error of the method and might suggest a drift of Envisat data with respect to tide gauges.

Global MSL studies attest to the particular behavior of the Envisat MSL, especially at the beginning of the altimeter time period (AVISO, 2013, Envisat annual validation report [3]). This seems to be consistent with the fact that the Envisat GMSL trend is higher than the Jason-1 one, and is also confirmed by the comparison to Argo floats (see *Validation of altimeter data by comparison with in-situ Argo T/S profiles*, 2013 annual report [6]). The number of tide gauge stations used in Envisat analysis is displayed on figure 16.

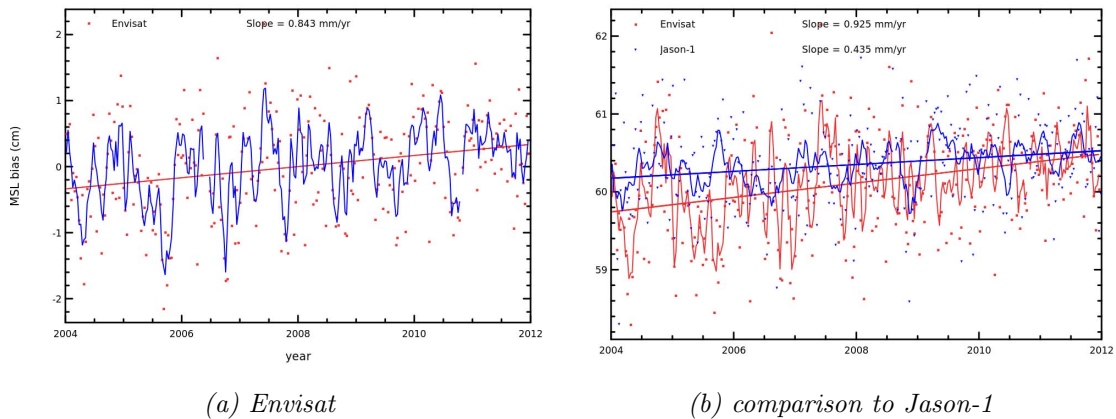


Figure 15: time series of the global average differences between Envisat and tide gauges (15a) alone, and compared to Jason-1 (15b)

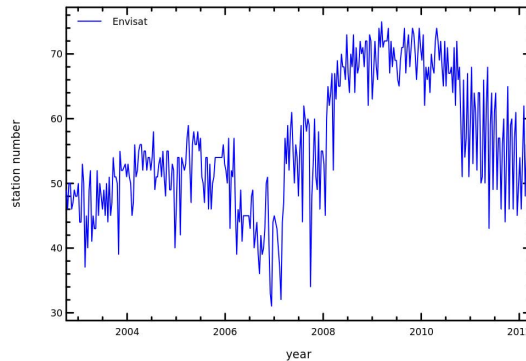


Figure 16: Temporal evolution of the number of tide gauges used in the estimation of global average differences between Envisat and in-situ records.

4.4. Analysis on multi-mission gridded datasets

Analysing multi-mission datasets provides a way to study long, homogeneous time series. In this section we present the activities performed over the last year regarding the comparison of the so-called "value added" products to in-situ SSH measurements from tide gauges.

4.4.1. SSALTO/DUACS maps of Sea Level Anomaly

The DUACS Delayed Time gridded products have been compared with tide gauges on the entire altimeter time period. Both multi-mission and mono-mission¹ products are studied in order to assess the reliability of the comparison with tide gauge measurements with or without combining altimeter data coming from different sensors.

On the 1993-2013 time period, no significant drift is observed, either for DUACS Delayed Time merged or mono-mission products (see figure 17), within the error of the method of $\pm 0.7 \text{ mm.yr}^{-1}$ (Ablain et al., 2009 [2]).

Amplitudes of SSH differences are of the same order except between September 2002 and October 2005 where the amplitude seems to be reduced with the combination of the four missions T/P, Geosat Follow-On, Jason-1 and Envisat. Furthermore, the standard deviation is quite low, with a mean value close to 0.6 cm for both multi-mission and mono-mission products. Therefore, the use of tide gauges measurements can also be considered as a way of assessing long-term drifts considering DUACS DT gridded products.

¹the mono-mission product refers to the optimal interpolation performed by DUACS using only one reference altimetry mission at a time (first Topex/Poséidon, than Jason-1 and now Jason-2) while the multi-mission product refers to delayed-time DUACS processing using all altimetry missions available.

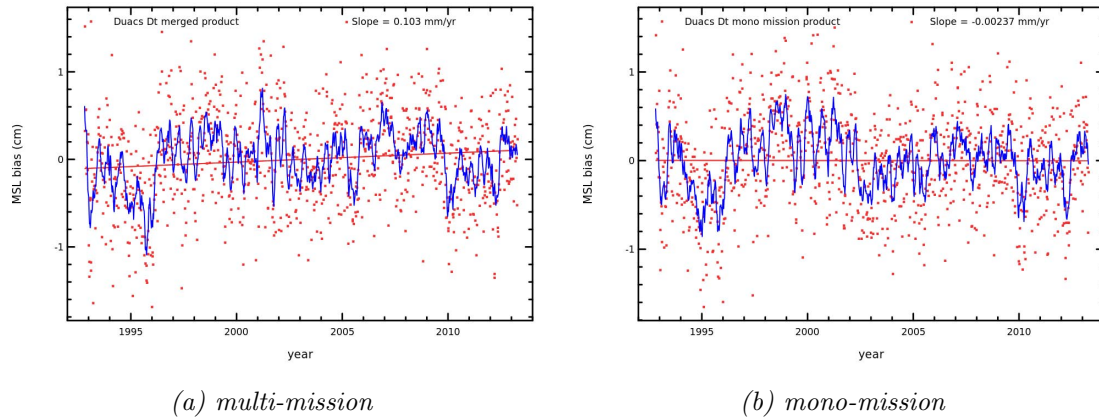


Figure 17: time series of global average differences between Duacs merged product (17a), Duacs mono-mission product (17b) and tide gauges data

4.4.2. ESA's Sea Level Climate Change Initiative dataset

This year was also performed a complete evaluation of the sea level grids computed within the framework of ESA's Climate Change Initiative project with respect to in-situ data, both tide gauges and Argo profiles. For this evaluation, a new approach has been used and the signals observed by satellite altimeters have been compared to in-situ sensors separating different time and space scales. The report summarizing the results is appended to the present document (see annex 10.2.).

5. Evaluation of new altimeter standards or methods

5.1. Overview

In addition to the ability to detect long-term drifts and jumps in satellite altimeter time series, in-situ records (both tide gauges and Argo profiles) provide an independent reference to assess the quality of new altimetry standards. The usefulness of in-situ data for such analyses has been demonstrated in the past (for example with the Envisat retracking evaluation).

This part of the document will focus on the impact of the GPD wet troposphere correction in the computation of TOPEX/Poseidon SSH and the use of the objective analysis in the level-2 SSH calculation when comparing to tide gauges.

5.2. Evaluation of the GPD wet tropospheric correction

The GPD wet tropospheric correction is a new algorithm based on GNSS path delays whose goal is to improve the quality of the wet tropospheric correction in coastal areas ([21]). An assessment of the impact of this correction on different missions has shown significant impacts on SSH derived from TOPEX/Poseidon, especially in the Indian Ocean. As an example, figure 18 displays the impact of this new correction on TOPEX/Poseidon SLA trends. Trend differences remain low (the colorbar ranges from -0.2 to 0.2 mm.yr^{-1}), yet it appears clearly that changes are concentrated in the Indian Ocean. We cannot expect to detect this level of SLA trends modifications with tide gauges data as uncertainties are too high, both on in-situ data in the region and on the comparison methodology, that's why we focused on the variance of SSH differences between altimetry and tide gauges.

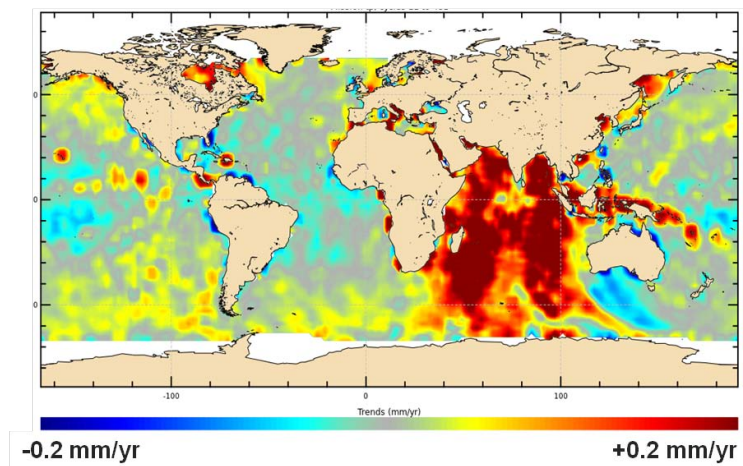


Figure 18: Impact of the GPD wet tropospheric correction on SLA trends (in mm.yr^{-1}) estimated from TOPEX/Poseidon data

As part of the performance assessment of this new wet tropospheric correction retrieval algorithm, we compared SSH from TOPEX/Poseidon estimated with the standard radiometer and the GPD wet tropospheric corrections to tide gauge measurements. The comparison focuses on the Indian

Ocean region, where the effects of the new correction are larger. Only 17 tide gauge stations have recorded SSH in this region and during this period, so the present study is performed on a rather small sample. Figure 19 displays the change in the variance of the altimetry minus tide gauge differences in the Indian Ocean. The variance reduction is represented as an histogram, negative values indicate that the variance of the differences between altimetry and tide gauge data is reduced when using the GPD correction, thus indicating a better consistency between the altimetry and in-situ records.

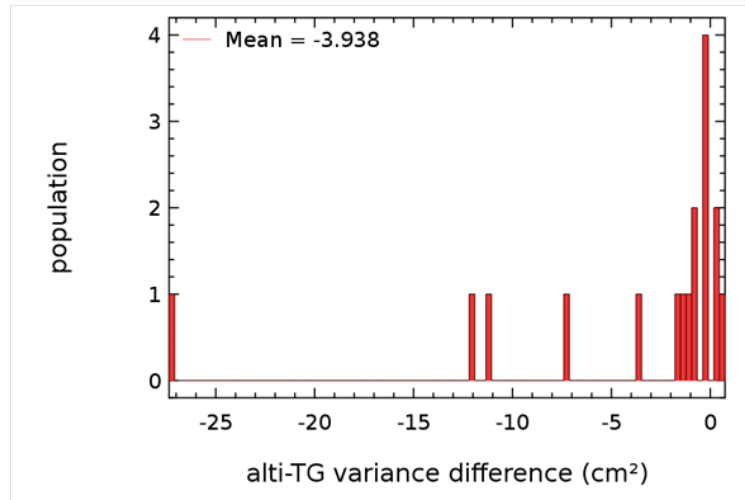


Figure 19: Histogram of altimetry minus tide gauge variance differences in the Indian Ocean

5.3. Impact of the objective analysis on altimeter/tide gauges comparisons

To better validate altimeter data with regard to in-situ measurements, it is interesting to use an objective analysis of the data so as to take the most widespread sample of tide gauges into account close to altimeter data. The effect of such objective analysis is measured in this study on Jason-1 and Jason-2 missions on their whole time period.

Figure 20 displays on the left the trend of the MSL bias while the right part shows the monitoring of the standard deviation and the number of tide gauges considered on Jason-1 mission. The main reliable result comes from the combination between those two plots. First the trend of SSH differences seems to be weakly impacted by the differences between along-track data or using an objective analysis on Jason-1 before the comparison with tide gauges. Results are thus in agreement within the error of the method (respectively 0.3 mm.yr^{-1} and 0.1 mm.yr^{-1} for the along-track data and the objective analysis). Moreover, the higher number of tide gauges considered in the comparison with the objective analysis and the lower mean of the standard deviation (3.1 cm vs 3.6 cm when using along-track data) are in favor of a better accuracy of the trend estimate of the MSL bias with an objective analysis.

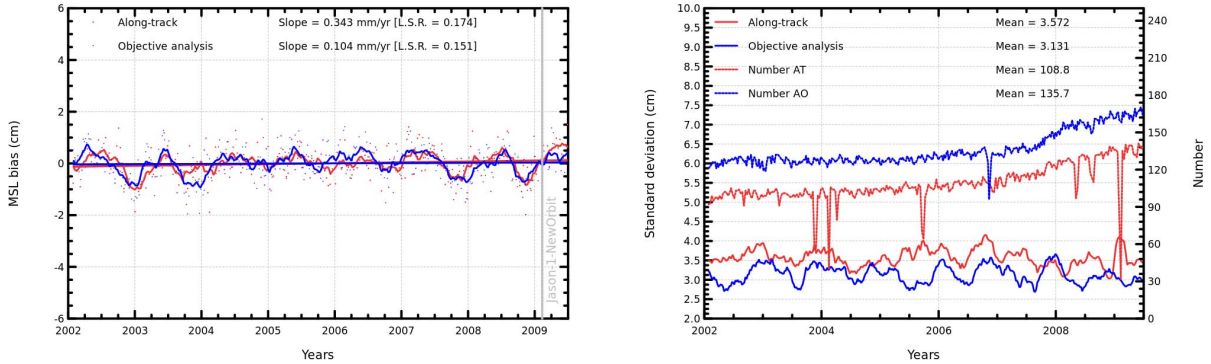


Figure 20: Left: Trend of the SSH differences between Jason-1 and tide gauge measurements considering level-2 data or an objective analysis. Right: Monitoring of the standard deviation and number of tide gauges considered using Jason-1 along-track data (AT) or an objective analysis (AO)

Focusing on the histogram of the standard deviation of trend differences (see figure 21), previous results are confirmed. The mean of the standard deviation of the trend differences is slightly weaker using an objective analysis, even if the same classes seems to appear on the histogram. The population of tide gauges is densier between 2 cm^2 and 6 cm^2 with the objective analysis whereas it is offset between 3 cm^2 and 7 cm^2 when considering along-track data. The conclusion for this study is that considering products derived from an objective analysis would bring a better reliability on the comparison between altimeter data and tide gauge measurements, either with a reduced error on the comparison itself or on the larger number of tide gauges considered.

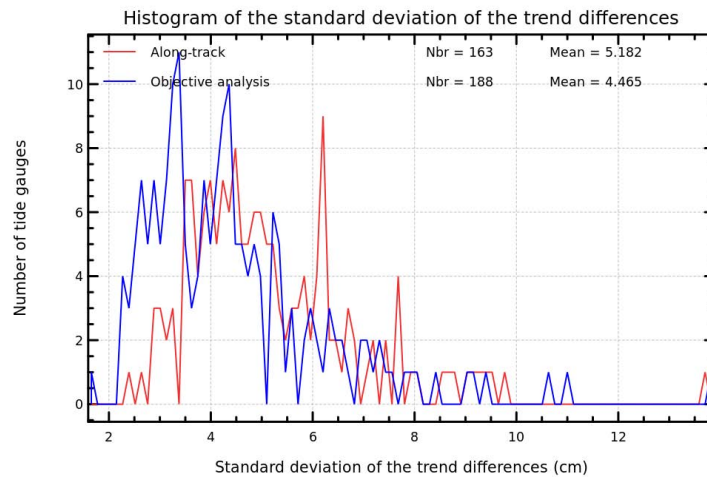


Figure 21: Histogram of the standard deviation of trend differences considering Jason-2 level-2 data or an objective analysis

6. Quality assessment of tide gauge time series

To complete the global assessment of altimeter data where in-situ measurements are used as independent sources of comparison, tide gauge networks are compared to altimeter SLA time series. This part aims at highlighting potential anomalies on in-situ time series:

- from the detection of structural changes in in-situ time series
- from comparisons with all available altimeter data

6.1. Detection of structural changes in in-situ time series

6.1.1. Position of the problem

Last year's annual report (ref. SALP-RP-MA-EA-22157-CLS) questioned the validity of the PSMSL quality flag. It showed that several PSMSL time series had very odd behaviours, such as jumps or important drifts, even if quality flag did not indicate any problem with the data. At that time, such behaviour could only be identified through a manual careful inspection of all time series, which represents an important workload given that the PSMSL dataset contains more than two thousand stations. The purpose of the work presented here was to investigate if a test could be designed to detect structural changes in sea level time series (the application field is wider than tide gauge time series only).

6.1.2. Methodology

For this work we adopted the framework of empirical fluctuation processes which is basically described below. A complete description can be found in Zeileis et al., 2003 [19] and Zeileis et al., 2010 [20]. Different tests for detecting structural changes in linear models are implemented in order to investigate regime shifts in time series, note that we used an R package named `strucchange`².

The basic idea behind those tests is to first construct a linear model linking an independent variable Y (in our case this is generally sea level) to a dependent variable X (in our case this is generally time). We chose to stick with very simple linear models

$$Y = a_1 X + a_0 + \epsilon_i \quad (2)$$

where the ϵ_i represent the deviation of Y from the linear model (*i.e.* the residuals). Once this model is fitted to the data, a number of quantiles can be evaluated such as

$$W(t) \propto \frac{1}{\hat{\sigma}\sqrt{n}} \sum_{i=1}^{\lfloor nt \rfloor} \hat{\epsilon}_i \text{ for } (0 \leq t \leq 1) \quad (3)$$

where W evolves over the time series length and is proportionnal to the cumulative sum of residuals. If there is a sudden change in the residuals behaviour, then this change should impact W . Another test relies on the estimation of a quantity named F_p :

$$F_p \propto \epsilon^\top \epsilon - \hat{\epsilon}(p)^\top \hat{\epsilon}(p) \quad (4)$$

²R is a free software environment for statistical computing (see <http://www.r-project.org/>) and the `strucchange` package is available at <http://cran.r-project.org/web/packages/strucchange/index.html>.

which compares the scalar products of the residuals estimated over the whole length of the time serie and over varying sub-segments p . Again, if the residuals of the linear model follow the same distribution over time, then the evaluation of $\hat{\epsilon}(p)^\top \hat{\epsilon}$ over each sub-segment p will not differ much from the value estimated over the whole period.

6.1.3. Results

These methods have been tested on time series of the differences between altimetry and tide gauges generated during the routine comparison of the Jason-1 mission with GLOSS/CLIVAR data. It should be noted that this structural change detection has only been performed on time series that are effectively used to generate the global average of differences between altimetry and tide gauges, so only on time series that successfully pass the quality check criteria.

In order to illustrate the kind of results that can be obtained with such methods, we show in this report the analysis of one time serie extracted at station Kushimoto situated along the coast of Japan. The time serie of the differences between Jason-1 and the Kushimoto tide gauge is displayed on figure 22. There is strange behaviour at the beginning of the time serie, and we can suspect two jumps in the time series leading to a portion of the differences in March 2010 (around CNES julian day 22000) being much lower.

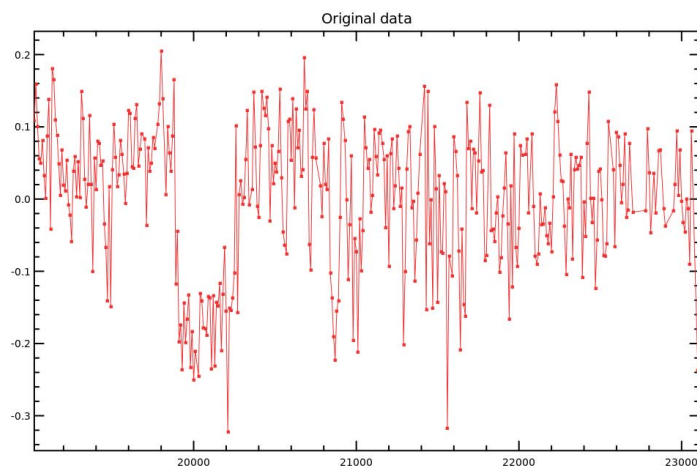


Figure 22: Time series of SSH differences between Jason-1 and the tide gauge at station Kushimoto

Applying the empirical fluctuation tests on this time series leads to the results displayed on figure 23, where the red lines represent the 95% significance level. From these two tests, a significant structure change is displayed over the time series, and this structural change is correlated to the bias observed on the time series.

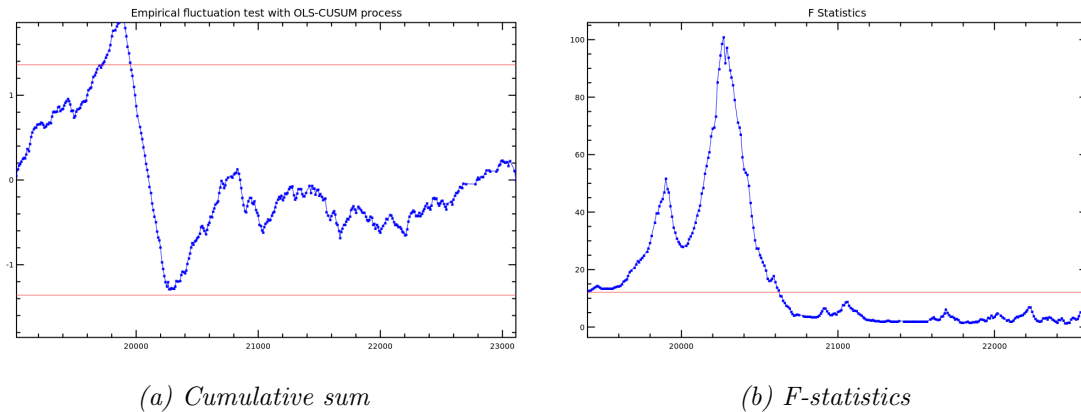


Figure 23: Two examples of the empirical fluctuation tests applied on the time series of figure 22

6.1.4. Conclusions and Futures

Results presented here are preliminary and further work is needed to build a reliable and automatic structural change detection test in altimeter and in-situ SSH time series. However, the first results are promising, and this statistical tools will be routinely used to strengthen the quality control applied on in-situ data and thus improve the reliability of the altimetry/tide gauges comparison processing.

6.2. A new design for in-situ information cards

The classical way to assess the quality of sea level time series recorded by tide gauges is to perform a comparison to satellite altimetry missions. Performing systematically such comparisons for each station in the network allows us to detect drifts and jumps in in-situ time series. For each station, the results of this quality assessment process are summarized on an in-situ information card. The aim of this card is to quickly represent the performance of the in-situ sensor with respect to satellite altimetry.

6.2.1. Description of the information cards

This year we developed a new design for the tide gauge information cards in order to enrich the information displayed with new metrics and diagnostics. The final goal is to provide a large number of criteria in order to facilitate the detection of a spurious behaviour in in-situ time series, at the cost of a slight increase in complexity. These new information cards are composed of the same type of information than the previous version, but with a different layout. An example of the new design of in-situ information cards is given in figure 24. The card is composed of several boxes whose content is described below:

- **General Information:** contains general information about the tide gauge station, its name and position, the station code, the station network and the number of satellite altimetry missions matching this station.
- **Statistics:** this section of the information card summarizes statistics estimated on the time series of the differences between altimetry and tide gauge data. The statistics considered

here are the correlation, the Taylor distance, the altimetry and tide gauge SSH standard deviation, the RMS of the differences, the trend of the differences and the uncertainty on this trend based on a Monte-Carlo simulation. The distance between the tide gauge position and the position where the satellite altimetry time series was extracted is also displayed.

- **Location Information:** this box contains two maps, a global one representing the position of the tide gauge station and a zoom centered around the tide gauge position where the positions of the satellite altimetry time series are extracted.
- **Taylor diagram:** the taylor diagram in this box uses the in-situ data as a reference, the color points therefore refer to the different altimetry missions considered,
- **Correlations:** this box displays the maps of the correlation coefficient between tide gauge and altimeter SSH, for each matching satellite altimetry mission.
- **Time Series:** this box contains two plots, one for the SSH from in-situ data and from matching satellite altimetry data, and one for the time series of the SSH differences between altimetry and in-situ data,
- **Seasonnal Cycle:** the seasonnal cycle is very often a dominant feature of sea level variability and it is useful to have a visual display of its shape,
- **Structural changes:** this is a direct application of the method described in section and intends to emphasize quickly potential structural changes in time series of SSH differences.

Since this release provides several new analyses, a simplified information card is expected to be designed and distributed along with the complete version. A proposal for this simplified version is available in this report as an annex (10.3.). Therefore, both versions of the in-situ information cards could be simultaneously available for end-users to provide these two levels of information.

As it is now, these new information cards will be routinely generated and distributed through the AVISO website on a weekly basis and allow for a quick overview of the tide gauge performance for the comparison with altimetry.

COMPARISONS BETWEEN ALTIMETRY AND TIDE GAUGE DATA
AT STATION MAJURO

generated on Wednesday 18th December, 2013 at 18:26:11

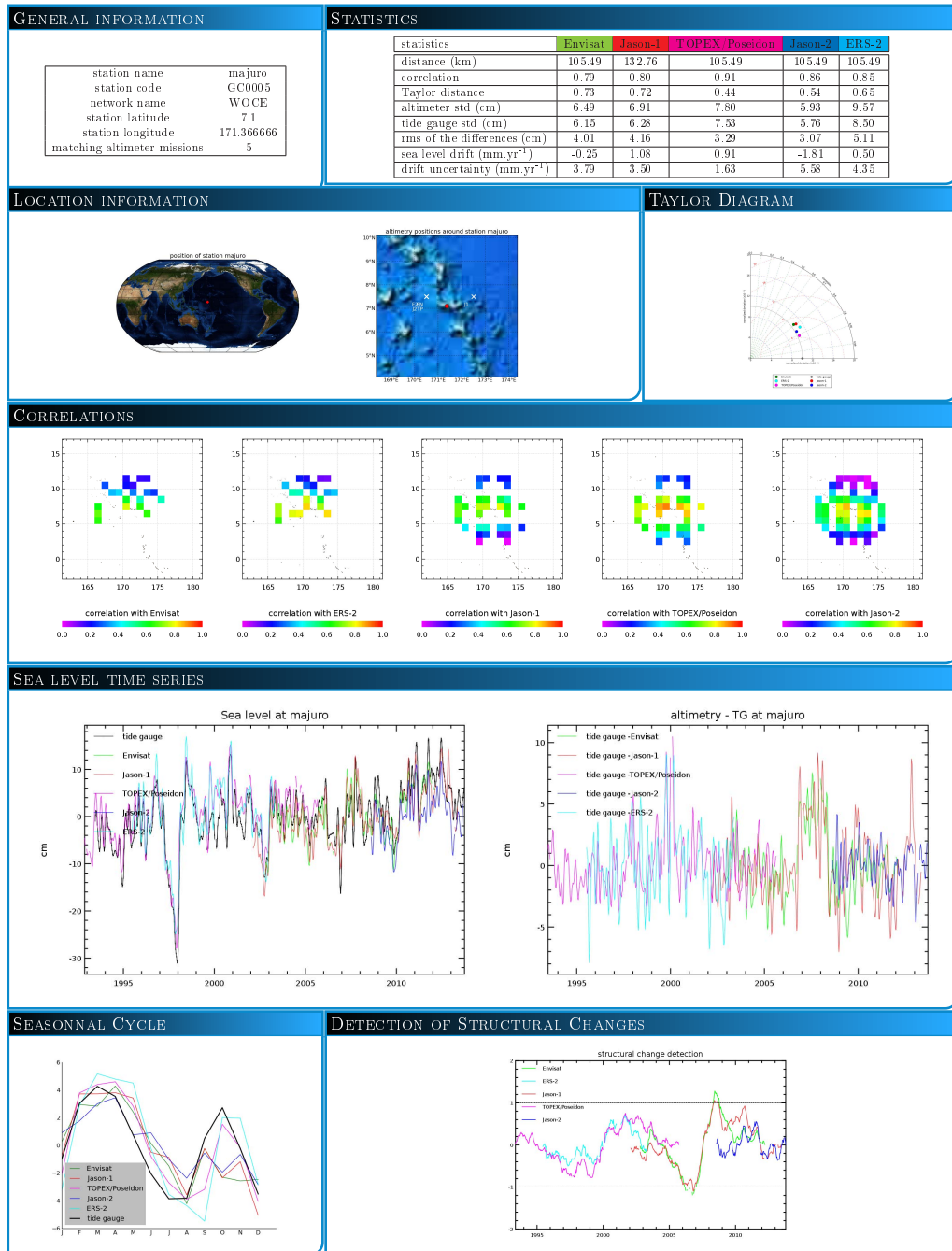


Figure 24: Example of a tide gauge information card

7. 2013 Particular Investigations

7.1. Accounting for GIA effects on altimetry data

The glacial isostatic adjustment (GIA) refers to the visco-elastic response of the earth's envelopes to the surface loading changes following the melting of large ice packs since the last glacial maximum (approximately twenty thousand years ago).

7.1.1. Theoretical elements

The GIA process affects the comparison between altimetry and in-situ measurements, and should be accounted for. However the correction to be applied is not the same on altimetry and tide gauge data.

Regarding tide gauge SSH measurements, the GIA is responsible for vertical motion of the earth's crust and therefore of the tide gauge datum. Vertical motion rates as large as several $mm.yr^{-1}$ can be found in some regions such as Northern Europe. The GIA also has an impact on the ocean surface and on the height measured by satellite altimetry through changes in ocean basin volume and geoid changes due to internal mass redistributions. Tamisiea et al. (2011, [16]) provide a review of the the different effects of GIA induced signal on sea level as measured by satellite altimetry and tide gauges.

Figure 25 is taken from their paper and displays the impact of GIA signals on present-day sea level as it would be measured by different type of instruments (both in-situ and remote sensors). The top panel represents the effect on sea level measured by tide gauges. This effect (which can be large in some regions) is currently accounted for in our processing by using relative sea level GIA rates predicted by the ICE5G_VM2 model (Peltier, 2004 [13]). The middle panel represents rates induced by GIA effects on sea level measured by satellite altimetry. The average of this map over the oceanic domain amounts to $-0.3 mm.yr^{-1}$, meaning that the global sea level rise rate is underestimated by satellite altimeters. This is generally corrected on global mean sea level estimates by adding $0.3 mm.yr^{-1}$ to the trend estimated from satellite altimeters, but figure 25 shows that this rate is not uniformly distributed over the ocean.

The question that the investigation presented here tends to answer is: "Does correcting satellite altimetry data for local GIA rates rather than a global one have an influence on the comparison between satellite altimetry and tide gauges ?"

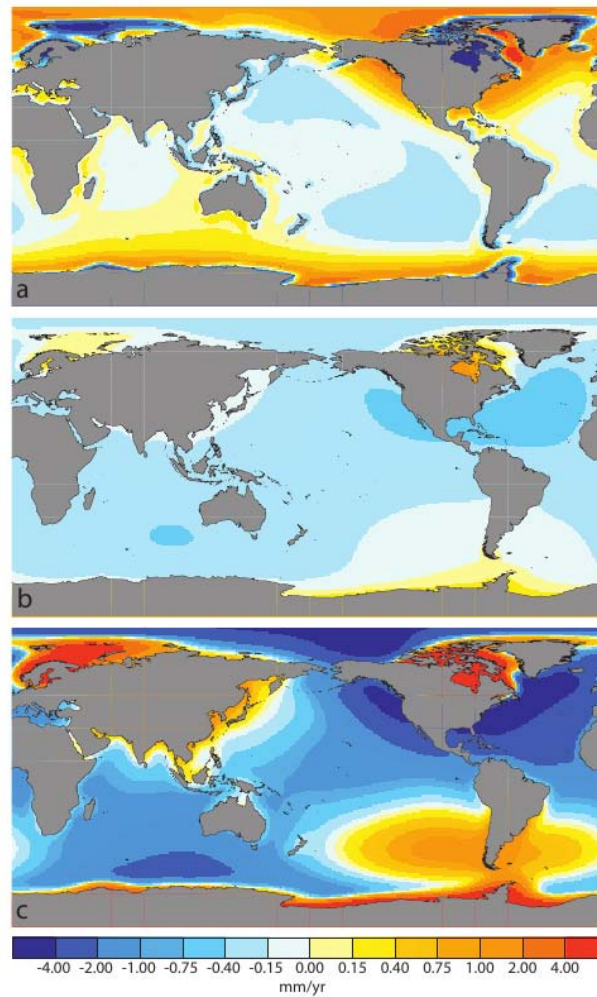


Figure 25: Numerical prediction of the rates induced by GIA on present day sea level change measured by tide gauges (top), satellite altimetry (middle) and by a gravity mission like GRACE (bottom).

7.1.2. Current strategy

In the current version of the processing, tide gauge time series are corrected for GIA effects on relative sea level measurements at the pre-processing level. The current strategy for correcting satellite altimetry measurements for GIA effects when comparing altimetry and tide gauges is to apply a -0.3 mm.yr^{-1} correction to the global average time series. This method relies on the assumption that the GIA effect on satellite altimetry SSH measurements is uniformly distributed over the whole oceanic domain.

In practice the -0.3 mm.yr^{-1} trend correction is applied at the very end of the processing, once the time series of global average differences between satellite altimetry and tide gauges is generated.

7.1.3. Alternate strategy

The alternate strategy is to correct satellite altimetry time series for the local effect of GIA as predicted by a model. We use the GIA model ICE5G_VM2 from Peltier, 2004 ([13]). The map of the GIA rates to be applied to altimetry data predicted by this model is presented on figure 26. Note that this figure is equivalent to the one shown on figure 25 (middle), but for a different model. For this experiment, satellite altimetry data were corrected after the pre-processing of the data by applying linearly over time the map of figure 26 to cycle by cycle box-averages of satellite SLA data.

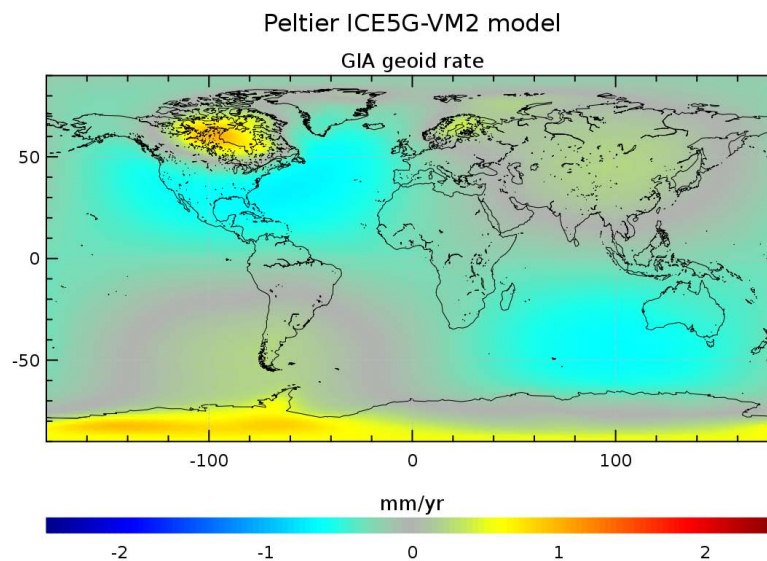


Figure 26: GIA correction to be applied to satellite altimetry SSH rates derived from the ICE5G/VM2 model.

7.1.4. Experiment

In order to evaluate the impact of correcting satellite altimetry time series for local GIA rates rather than the global mean rate on the comparison to tide gauge data, an analysis is performed over the TOPEX/Poseidon, Jason-1 and Jason-2 time periods. The advantage of using the longest period for the analysis is to emphasize the impact of the GIA correction change, which should modify only long-term trends.

For this experiment two comparisons between the same GLOSS/CLIVAR tide gauge dataset and satellite altimetry are performed:

- one where is applied a uniform GIA rate on satellite altimetry data (*i.e.* the current strategy),
- one where local GIA rates derived from the model are applied (*i.e.* the alternate strategy).

Results obtained from these two runs are then compared to evaluate the impact of the change in the GIA rate correction on altimeter data.

7.1.5. Results

Figure 27 displays the two time series of the global average differences between satellite altimetry and tide gauges obtained with the current and alternate strategy for correcting GIA induced rates on satellite data.

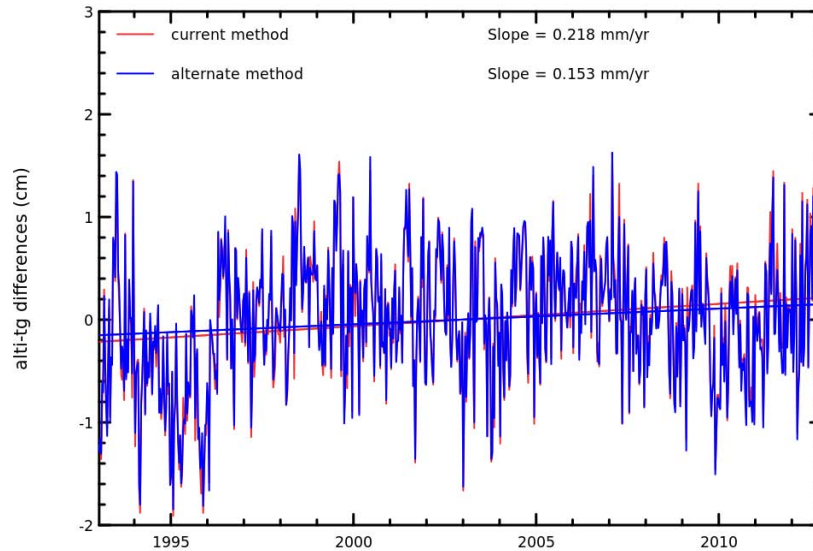


Figure 27: Time series of global average differences between altimetry and tide gauges using the current (red) and alternate (blue) methods for correcting GIA signals on altimetry data.

Over the in-situ data sample used for this test, applying a uniform -0.3 mm.yr^{-1} GIA rate to altimetry tends to over estimate the GIA contribution. Over the whole period studied here, without any GIA applied to altimetry the global average drift between altimetry and in-situ data amounts to -0.08 mm.yr^{-1} . This drift is changed to 0.22 mm.yr^{-1} when applying the uniform drift to altimetry data, a value larger than the 0.15 mm.yr^{-1} drift obtained when using local GIA rates to correct altimetry data.

We also performed the same kind of test using Envisat data. Although time series are shorter, Envisat's densier data coverage at high latitudes could be more impacted by this GIA change than TOPEX like missions, because large values of GIA rates are found at such latitudes. For Envisat, comparisons show that the impact of correcting altimetry data for local GIA rates has a larger impact, at about 0.15 mm.yr^{-1} .

Even if there is little effect on the global average trend, we can investigate station-wise statistics. Figure 28 displays the histogram of the trend differences between satellite altimetry and tide gauge data evaluated at each station, for different analysis and corrections of GIA induced SSH variations on altimetry and tide gauges. Correcting for GIA effects using a local rate rather than a global one results in a better centering of the histogram, however the standard deviation of the trend differences is not reduced. For Envisat data, the centering of the histogram is unchanged and the standard deviation of trend differences is reduced, but only by about 0.2 mm.yr^{-1} .

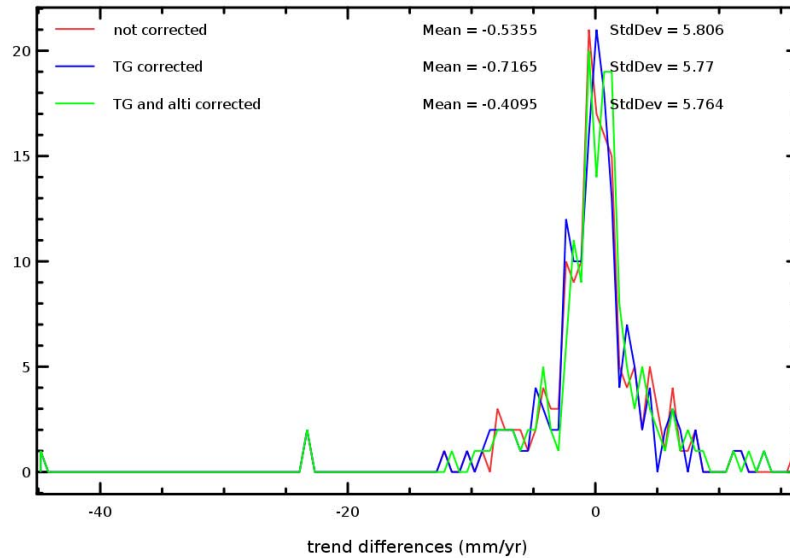


Figure 28: Histogram of trends of the differences between altimetry and tide gauge data, without any GIA correction (red), with tide gauges corrected for GIA (blue), and with tide gauges and altimetry corrected for GIA signals (green).

7.1.6. Conclusions

Correcting satellite altimetry data for local GIA rates rather than a uniform one has a little impact on the comparisons to tide gauge measurements: 0.07 mm.yr^{-1} on the Topex/Jason-1/Jason-2 experiment and 0.15 mm.yr^{-1} on the Envisat test. Results obtained over the years using the global average value of 0.3 mm.yr^{-1} would not be significantly modified by the new correction strategy presented here. However, it is theoretically more consistent to correct satellite altimetry for local GIA rates rather than the global one, and not doing it induces an error on the drift evaluation which is around $0.1 \sim 0.2 \text{ mm.yr}^{-1}$ but might depend on the tide gauge network distribution and may be more important for regional studies.

7.2. Comparing the new GeoSat dataset with tide gauge measurements

The U.S. Navy GEOSAT altimetric mission was the first mission to provide global data over a long period (from 1985 to early 1990). While Geosat was on a geodetic orbit during the first 18 months, it was moved on a 17-day exact repeat track since November 1986. Although the dataset is less precise than recent altimeter datasets such as Jason-2, the Geosat data are interesting as they are the only available global altimeter data before the 1990's.

The goal of this study is to compare the new release of the 1Hz GeoSat dataset with tide gauge measurements. This new version of the GeoSat products is supplied by the RADS database (<http://rads.tudelft.nl/rads/rads.shtml>), which contains the new geophysical standards such as ionospheric model, wet and dry tropospheric correction from models, but also the recent release of precise orbit ephemeris from the National Aeronautics and Space Administration (GSFC 0905).

7.2.1. Results

To perform this study, the MOG2D dynamical atmospheric correction has been computed on the GeoSat time period. Thanks to such processing, the SSH derived from tide gauge measurements is computed and the comparison to altimeter data is performed with the standards of the new release (see annex 10.4.).

The first part of the study focuses on the 1985-1990 altimeter time period. Processing the comparison between both datasets results in discrepancies when calculating the correlations between altimeter and in-situ time series. Figure 29 displays the non-homogeneous evolution of the number of tide gauges along the time period, which is coherent with the change in the repetitivity of the altimetric mission. Indeed the maximum of tide gauges considered happen at the beginning of the repetitive orbit. This number of tide gauges, close to 80, is almost stable until the altimeter begins to lose some data. Next to such results, the comparison to tide gauges measurements is performed from the beginning of the repetitive period to this data loss, marked as "End of study time period" on the figure.

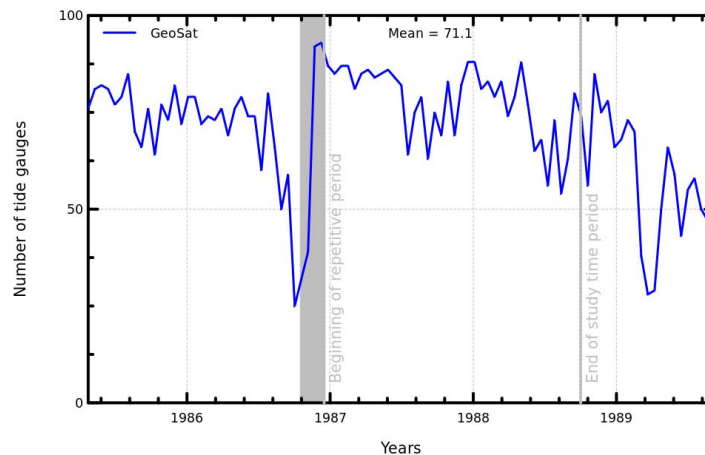


Figure 29: Number of GLOSS/CLIVAR tide gauges considered in the comparison with GeoSat between 1985 and 1990.

Thus, figure 30 shows the comparison between GeoSat new release with tide gauge measurements on the repetitive period of the mission. Although the trend of the SSH differences cannot be considered as reliable over this short time period, it is close to -1.6 mm.yr^{-1} (figure 30 left). Naturally, the formal adjustment error is quite large (2.5 mm.yr^{-1}), again explained by the short period considered. However, when looking at figure 30 right, the mean of standard deviation of the differences is lower than 4 cm and stable on the studied period of the altimeter, with a number of tide gauges sufficient to compute such kind of statistics (close to 90 in average, figure 30 right).

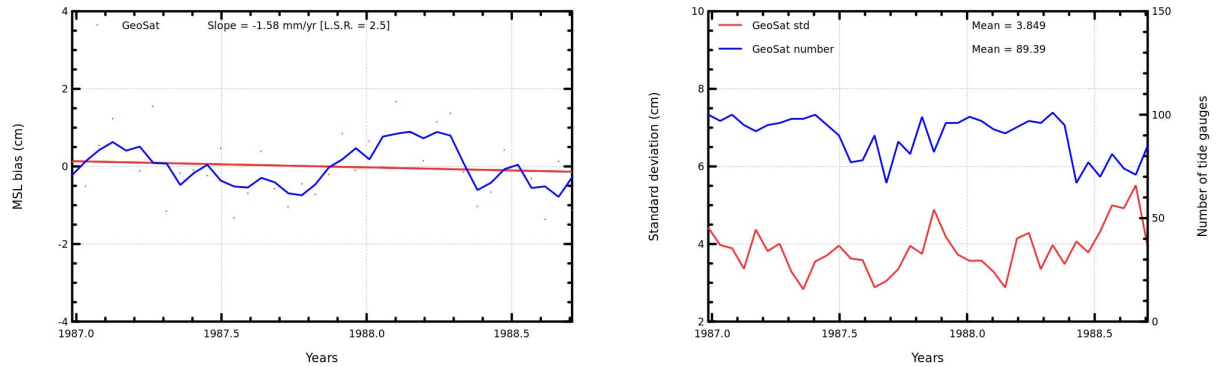


Figure 30: Left: Trend of SSH differences between GeoSat and tide gauges on the repetitive orbit (mm/yr). Right: Standard deviation (red curve) and number (blue curve) of the comparison between GeoSat's repetitive orbit data and GLOSS/CLIVAR tide gauge measurements.

7.2.2. Conclusion

While the comparison between GeoSat's new dataset with tide gauge measurements cannot be considered as reliable to date, preliminary results show that both datasets can be comparable. To go further in the study and try to extend the global MSL trend to GeoSat's time period, it will be interesting to consider the whole altimeter records in the comparison with tide gauge measurements. However, because of the different phases of the mission (geodetic vs repetitive) and the increase of data loss since November 1988, the methodology of comparison should have to be specifically adapted.

8. Conclusions

This report presents the operating result of the altimeter/tide gauges comparison processing. As an operational component of the altimeter calibration/validation activity (development and operational account, automatic processing, ...), reliable results from the comparison to tide gauge measurements are compiled thanks to an homogeneous tidal database and a robust methodology to assess potential drifts or jumps in the altimeter measurements. Therefore, the processing sequence is routinely performed in the whole studies involving altimeter data in order to better benefit from the external and independent comparison with tide gauge measurements and improve the relevance of analyses.

In 2013, the tide gauge database has been renewed to better acquire GLOSS/CLIVAR hourly as well as PSMSL monthly time series, aiming at dependable climate applications. From now on, two databases are available. While the first one concerns the download and the storage of the raw data in CLS format, the second one is dedicated to the comparison with altimetry, updated with different standards (oceanic tide, land motion, ...) in order to get fully post-processed tide gauge measurements. These new databases are fully operational and new in-situ datasets will be added to improve the global sampling for reliable studies about long-term sea level variability, globally and regionally.

Concerning the accuracy of altimeter data, both improvements on the data acquisition and investigations with regard to the comparison procedure have reinforced results on the main altimeter missions:

- Both Jason-1 and Jason-2 missions provides consistent long-term trend differences when compared to tide gauge measurements, and no MSL drift is detected, within the error of the method estimated to 0.7 mm/year over the altimeter time period
- Concerning Envisat space mission, SSH differences with tide gauges highlight a drift of almost 0.8 mm/year, in line with global MSL studies which attest to the particular behavior of the Envisat MSL, especially at the beginning of the period (AVISO, 2013, Envisat annual validation report [3])
- The global trend of SSH differences between TOPEX/Poseidon (T/P) data and tide gauge measurements is about 0.6 mm/year over the 1993-2005 time period. Although it provides accurate measurements for climate studies, the comparison with in-situ data demonstrates the need for this altimeter mission to be reprocessed, in particular to improve the long-term stability of TOPEX-A data
- Looking at SSALTO/DUACS maps of sea level anomaly, no significant drift is observed on the 1993-2013 time period when comparing to tide gauges, either for DUACS Delayed Time merged or mono-mission products

Moreover, these results are in agreement with global Calval studies, which reinforced the idea of using independent in-situ tide gauge measurements is a way of getting an assessment of the error on the global MSL trend.

.....

The second part of this activity concerns the impact of new altimeter standards as a consequence of global or regional drifts detected on altimeter time series. In order to attest to some potential improvements of altimeter products for end-users, their impact in the sea level computation can be assessed thanks to tide gauge measurements. For instance, the GPD wet tropospheric correction has been assessed on different missions and has shown significant impacts on SSH derived from T/P, especially in the Indian Ocean. Furthermore, the impact of the objective analysis on altimeter/tide gauges comparison has been studied on Jason-1 and demonstrates the better accuracy of the trend estimate of the MSL bias using such altimeter processing, with an increased number of tide gauges taken into account.

The third part of this activity concerns the way the method presented here can provide a quality assessment on both altimeter and in-situ datasets through SSH comparisons. First, a method has been developed to automatically detect structural changes in sea level time series instead of a manual careful inspection of all time series. Even if further work is needed to build a reliable detection test in altimeter and in-situ SSH time series, the first results are promising and this statistical tools will be routinely used to strengthen the quality control applied on in-situ data. Besides, the quality assessment of in-situ measurements can also be assessed using multiple altimeter time series. These multi-mission comparisons enable to point out drifts or jumps in in-situ time series, which need to be corrected to improve the coherence between both datasets. This quality control then provide reliable datasets of in-situ measurements, which are relevant to detect potential altimeter drifts or jumps and to estimate the quality of new altimeter standards.

To date, cross-comparison indicators are displayed as information cards for the GLOSS/CLIVAR network, which are routinely performed each week and distributed on the AVISO website (http://www.aviso.altimetry.fr/produits/sea_level/altimetry_calibration_and_validation/in-situ-global-statistics.html). Considering this webpage, a new dynamic interface is planned instead of the current tide gauge google map. This improvement follows on from the need for end-users to access and combine the multiple information available at CLS. In line with this interface, a new design for the tide gauge information cards has been developed this year to enrich the information displayed and thus provide a large number of criteria for the tide gauge quality assessment. However, cross-comparison indicators will remain unchanged and still allow for a quick overview of the tide gauge performance for the comparison with altimetry.

Furthermore, it is important to underline the synergy of both tide gauges and Argo in-situ datasets to assess the quality of altimeter data (Valladeau et al., [17]). Indeed, while tide gauge measurements provide long time series but a limited spatial sampling, Argo T/S profiles cover the global ocean on a shorter time period. Other kinds of in-situ instruments such as gliders (Bouffard et al., 2010 [7]) can be considered to perform comparison with altimeter sea level provided that physical contents are corresponding. The duality of these both types of data will constitute an asset for the calibration of future space missions as the Sentinel-3 mission (sentinelle3.com) or the Surface Water Ocean Topography (SWOT) mission (swot.jpl.nasa.gov). It will also be of great interest to assess improvements of reprocessed altimeter data such as time series of ERS-1&2 (ESA REAPER project). Thanks to the cross-comparison between results provided by the different approaches, the assessment of the MSL drift is more and more reliable and accurate, globally as well as regionally.

Note that this activity has been presented this year at the so-called "Journées REFMAR" workshop in Paris [18], at the ESA Living Planet Symposium in Edimbourg [15] and at the OSTST in Boulder [12]. Moreover, a collaboration with M. Saraceno from the CIMA (Centro de Investigaciones del Mar y de la Atmosfera) has been set up to compare the annual component of sea level variability computed at tide gauge locations with gridded multi-mission altimeter products (Ruiz et al., [14]).

Finally, next to OSTST recommendations, several studies will be performed in 2014 to compare methodologies and results from the different contributors to the assessment of altimeter performances using tide gauge measurements. These studies will mainly focus on sensitivity tests to estimate if differences between groups are statistically significant and from which processing steps they arise.

9. References

References

- [1] Ablain, M., S. Philipps, M. Urvoy, N. Tran, and N. Picot, 2012: Detection of long-term instabilities on altimeter backscatter coefficient thanks to wind speed data comparisons from altimeters and models. *Marine Geodesy* 2012, DOI: 10.1080/01490419.2012.718675.
- [2] Ablain, M., A. Cazenave, G. Valladeau, and S. Guinehut, 2009: A new assessment of global mean sea level from altimeters highlights a reduction of global trend from 2005 to 2008. *Ocean Sci. Disc.*, 6, 31-56.
- [3] AVISO, 2013: Envisat RA2/MWR ocean data validation and cross-calibration activities. 2013 annual validation report. SALP-RP-MA-EA-XXXXX-CLS ed. 1.0, 129 pp.
- [4] AVISO, 2013: Jason-2 validation and cross calibration activities. 2013 annual validation report. SALP-RP-MA-EA-22270-CLS ed. 1.0.
- [5] Bessero, G., 1985: *Marées*, Service Hydrographique et Océanographique de la Marine, Brest.
- [6] Legeais, J.F., and P. Prandi, 2013: Validation of altimeter data by comparison with in-situ Argo T/S profiles. SALP-RP-MA-EA-22281-CLS ed. 1.0.
- [7] Bouffard, J., A. Pascual, S. Ruiz, Y. Faugère, and J. Tintoré, 2010: Coastal and mesoscale dynamics characterization using altimetry and gliders: A case study in the Balearic Sea. *J. Geophys. Res.*, 115, C10029, doi:10.1029/2009JC006087.
- [8] Carrère, L. and F. Lyard, 2003: Modeling the barotropic response of the global ocean to atmospheric wind and pressure forcing - comparisons with observations. *Geophys. Res. Lett.*, Vol. 30, 1275, 4 pp. doi:10.1029/2002GL016473.
- [9] Cartwright, D.E., and A.C. Eden, 1973: Corrected Tables of Tidal Harmonic, *Geophys. J. R. Astr. Soc.*, 17 (5), 619-622.
- [10] Dorandeu, J., and P.-Y. Le Traon, 1999: Effects of global mean atmospheric pressure variations on mean sea level changes from Topex/Poseidon, *J. Atmos. Oceanic Technol.*, 16, 1279-1283.
- [11] Labroue, S., 2007 : RA2 ocean and MWR measurement long term monitoring, 2007 report for WP3, Task 2 - SSB estimation for RA2 altimeter. Contract 17293/03/I-OL. CLS-DOS-NT-07-198, 53pp. CLS Ramonville St. Agne

- [12] Prandi, P., G. Valladeau, J.F. Legeais, M. Ablain, and N. Picot, 2013: Analyses of altimetry errors using in-situ measurements: tide gauges and Argo profiles. OSTST, Boulder.
- [13] Peltier, W. R., 2004: Global Glacial Isostasy and the surface of the ice-age earth: the ICE-5G (VM2) Model and Grace. *Annu. Rev. Earth Planet. Sci.*, 32 (2004), pp. 111-149.
- [14] Ruiz Etcheverry, L. A., M. Saraceno, A. R. Piola, G. Valladeau, and O. O. Möller: Annual cycle in coastal sea level from gridded satellite altimetry and tide gauges. *Continental Shelf Research*, in press.
- [15] Valladeau, G., J.F. Legeais, M. Ablain, P. Prandi, N. Picot, P. Femenias, and J. Benveniste, 2013: Analyses of altimetry errors using in-situ measurements: tide gauges and Argo profiles. *ESA Living Planet Symposium*, Edimbourg.
- [16] Tamisiea, M.E., and J.X. Mitrovica, 2011: The moving boundaries of sea level change: Understanding the origins of geographic variability. *Oceanography* 24(2):24–39.
- [17] Valladeau, G., J.F. Legeais, M. Ablain, S. Guinehut, and N. Picot, 2012: Comparing altimetry with tide gauges and Argo profiling floats for data quality assessment and Mean Sea Level studies. *Marine Geodesy* 2012, DOI: 10.1080/01490419.2012.718226.
- [18] Valladeau, G., L. Soudarin, M. Gravelle, G. Wöppelmann, and N. Picot, 2013: Quality assessment of altimeter and tide gauge data for Mean Sea Level and climate studies.
- [19] Zeilis, A., C. Kleiber, W. Krämer, and K. Hornik, 2003: Testing and dating of structural changes in practice. *Computational Statistics & Data Analysis* 44 (2003) 109 – 123.
- [20] Zeilis, A., A. Shah and I. Patanaik, 2010: Testing, monitoring and dating structural changes in exchange rate regimes. *Computational Statistics & Data Analysis* 54 (2010) 1696 – 1706.
- [21] ESA Sea Level CCI Validation Report, WP2700 Coastal areas, 2011 http://www.esa-sealevel-cci.org/webfm_send/186.

10. Annexes

10.1. Annex: Corrections applied for altimeter SSH calculation

All the corrections applied on SSH for TOPEX/Poseidon, Jason-1, Jason-2 and Envisat space altimetric missions are summarized in the following table:

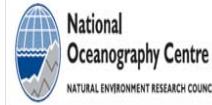
| Orbits and corrections | TOPEX/Poseidon | Jason-1 | Jason-2 | Envisat |
|--------------------------------|--|--|--|---|
| Orbit | GSFC POE (09/2008), ITRF2005+Grace | CNES POE (GDR-C standards until cycle 374, GDR-D standards from cycle 500 onwards) | CNES POE (GDR-D standards) | CNES POE (GDR-C standards) |
| Mean Sea Surface (MSS) | MSS CNES/CLS 2011 | MSS CNES/CLS 2011 | MSS CNES/CLS 2011 | MSS CNES/CLS 2011 |
| Dry troposphere | ECMWF model computed | ECMWF model computed | ECMWF model computed | ECMWF model computed |
| Wet troposphere | TMR with drift correction [Scharroo et al. 2004] and empirical correction of yaw maneuvers [2005 annual validation report] | Jason-1 radiometer (JMR) | Jason-2 radiometer (AMR) | MWR (corrected from side lobes) + new corrected files |
| Ionosphere | Filtered dual-frequency altimeter range measurements (for TOPEX) and Doris (for Poseidon) | Filtered dual-frequency altimeter range measurements | Filtered dual-frequency altimeter range measurements | Dual-Frequency updated with S-Band SSB (< cycle 65) GIM model + global bias of 8 mm (>= cycle 65) |
| Sea State Bias | Non parametric SSB (for TOPEX), BM4 formula (for Poseidon) | Non parametric SSB (GDR product) | Non parametric SSB (GDR product) | Updated homogeneous to GDR-C (Labroue, 2007 [11]) |
| Ocean and loading tides | GOT4.7 (S1 parameter is included) | GOT4.7 (S1 parameter is included) | GOT4.8 | GOT4.7 (S1 parameter is included) |
| Solid Earth tide | Elastic response to tidal potential [Cartwright and Tayler, 1971] [Cartwright and Edden, 1973] | Elastic response to tidal potential [Cartwright and Tayler, 1971] [Cartwright and Edden, 1973] | Elastic response to tidal potential [Cartwright and Tayler, 1971] [Cartwright and Edden, 1973] | Elastic response to tidal potential [Cartwright and Tayler, 1971] [Cartwright and Edden, 1973] |
| | | | | .../... |

| Orbits and corrections | TOPEX/Poseidon | Jason-1 | Jason-2 | Envisat |
|--|---|---|---|---|
| Pole tide | [Wahr,1985] | [Wahr,1985] | [Wahr,1985] | [Wahr,1985] |
| Combined atmospheric correction | High Resolution Mog2D Model [Carrère and Lyard, 2003] + inverse barometer computed from ECMWF model (rectangular grids) | High Resolution Mog2D Model [Carrère and Lyard, 2003] + inverse barometer computed from ECMWF model (rectangular grids) | High Resolution Mog2D Model [Carrère and Lyard, 2003] + inverse barometer computed from ECMWF model (rectangular grids) | High Resolution Mog2D Model [Carrère and Lyard, 2003] + inverse barometer computed from ECMWF model (rectangular grids) |
| Specific corrections | Doris/Altimeter ionospheric bias, TOPEX-A/TOPEX-B bias and TOPEX/Poseidon bias | Jason-1 / T/P global MSL bias | Jason-2 / T/P global MSL bias | USO correction included in the range after V2.1 reprocessing + PTR ³ |

Table 1: Corrections applied for altimetric SSH calculation

³External corrections available on ESA website near V2.1 GDR products

10.2. Annex: Evaluation of the Sea Level CCI dataset with respect to in-situ data



ESA Sea Level CCI

Validation Report: WP4XXX Altimetry validation with respect to in-situ data

Reference: CLS-DOS-NT-12-59

Nomenclature: SLCCI-VR-57

Issue: 1. 2

Date: Nov. 26, 12





| Chronology Issues: | | | |
|--------------------|------------|--------------------|-----------|
| Issue: | Date: | Reason for change: | Author |
| 1.0 | Nov. 26 11 | Initialization | P. Prandi |
| | | | |
| | | | |
| | | | |
| | | | |
| | | | |

| People involved in this issue: | | |
|--------------------------------|----------------------|--------------------------------|
| Written by (*): | P. Prandi, V. Pignot | Date + Initials:(visa or ref) |
| Checked by (*): | | Date + Initial:(visa ou ref) |
| Approved by (*): | | Date + Initial:(visa ou ref) |
| Application authorized by (*): | ESA | Date + Initial:(visa ou ref) |

**In the opposite box: Last and First name of the person + company if different from CLS*

| Index Sheet: | |
|--------------|---------------------------------|
| Context: | Baghera tool, project ACT-OCEAN |
| Keywords: | Oceanography, sea level |
| Hyperlink: | |

| Distribution: | | |
|---------------|-----------------------|-------|
| Company | Means of distribution | Names |
| CLS | Notification | |



List of tables and figures

List of tables:

| | |
|---|---|
| Table 1 : Global Mean Sea Level trends evaluated from altimetry data and in-situ measurements (all trends are expressed in $\text{mm}\cdot\text{yr}^{-1}$) | 4 |
| Table 2: SLA trend differences (mm/yr) between altimetry and in-situ estimated over different oceanic basins..... | 7 |

List of figures:

| | |
|---|----|
| Figure 1: Time series of the global mean SLA from tide gauges and collocated altimetry (left) and from altimetry and Argo profiles (right), the differences time series are artificially translated vertically. | 3 |
| Figure 2: Coherence diagram between altimetry and tide gauges (left), and between altimetry and Argo floats (right) for the global mean SLA time series | 3 |
| Figure 3: Time series of the inter-annual variability of the global mean SLA from tide gauges (left) and Argo profiles (right), and the corresponding co-located altimetry..... | 5 |
| Figure 4: Global mean SLA annual cycle estimated from tide gauges and Argo T/S data, and the corresponding co-located satellite altimetry (95% confidence levels for the monthly mean are overlaid as thin grey lines for the in-situ estimates) | 5 |
| Figure 5: Time series of the high frequencies of the SLA from tide gauges (left) and Argo profiles (right), and the corresponding co-located altimetry. The time series of the differences are represented in black with an artificial vertical shift. | 6 |
| Figure 6: Taylor diagram comparing altimetry (grey dot), tide gauges (triangles) and Argo profiles (circles) for the raw signal(black), the inter-annual signal (red) and the annual cycle (blue) and the high frequencies of the SLA (green) | 7 |
| Figure 7: Taylor diagram comparing tide gauges (triangles) and Argo profiles (circles) for the inter-annual signal of the ocean-basin wide averages of SLA over the Pacific Ocean (red), the Atlantic Ocean (blue) and the Indian Ocean (green). The global mean is represented in black..... | 8 |
| Figure 8: Basin-wide average SLA annual cycle for altimetry and tide gauge data for the Pacific Ocean (left), the Atlantic Ocean (center) and the Indian Ocean (right) | 9 |
| Figure 9: Basin-wide average SLA annual cycle for altimetry and Argo data for the Pacific Ocean (left), the Atlantic Ocean (center) and the Indian Ocean (right) | 9 |
| Figure 10: Taylor diagram comparing tide gauges (triangles) and Argo profiles (circles) for the high frequencies of the basin-wide mean SLA over the Pacific Ocean (black), the Atlantic Ocean (red) and the Indian Ocean (blue) | 10 |
| Figure 11: Coherence diagram between tide gauges and co-located altimetry (left) and Argo profiles and co-located altimetry (right) data for the high frequencies of the Pacific (red), Atlantic (blue) and Indian (green) oceans..... | 10 |
| Figure 12: Map of the SLA differences trends between altimetry and tide gauges (left) and between altimetry and Argo profiles (right)..... | 11 |
| Figure 13: Histograms of the trend differences (in mm/yr) between tide gauges and co-located altimetry (left) and Argo profiles and co-located altimetry (right) | 11 |
| Figure 14: Map of the inter-annual SLA variance differences between altimetry and tide gauges (left) and between altimetry and Argo profiles (right) | 12 |



Figure 15: Maps of the annual cycle amplitude (left) and phase (right) differences between SLCCI altimetry and tide gauges..... 12

Figure 16: Maps of the annual cycle amplitude (left) and phase (right) differences between SLCCI altimetry and Argo profiles 13

Figure 17: Map of the SLA variance differences between altimetry and tide gauges records (left) and between altimetry and Argo profiles (right) for the high frequency part of the signal 13

Figure 18: Time series of the global mean SLA estimated from the SLCCI (blue) and PVA (red) satellite altimetry datasets..... 14

Figure 19: Maps of the SLA trend differences between CCI and SALTO/DUACS datasets, estimated over the 1993-2010 (left) and 2003.5-2010 (right) periods 16

Figure 20: Map differences between trend differences between altimetry and Argo profiles evaluated with CCI and SALTO/DUACS altimetry datasets..... 16

Figure 21: Time series of hemispheric SLA (west left and east right) from Argo profiles (red) and co-located altimetry from CCI (red) and SALTO/DUACS (blue) 16

List of items to be confirmed or to be defined

Lists of TBC:

Aucune entrée de table des matières n'a été trouvée.

Lists of TBD:

Aucune entrée de table des matières n'a été trouvée.

Applicable documents

AD 1 Sea level CCI project Management Plan
CLS-DOS-NT-10-013

Reference documents

RD 1 Manuel du processus Documentation
CLS-DOC



List of Contents

| | |
|--|-----------|
| 1. Introduction | 1 |
| 1.1. Data description | 1 |
| 1.2. Data comparison methods | 1 |
| 1.2.1. Tide gauges | 1 |
| 1.2.2. Argo profiles | 2 |
| 1.3. Description of work | 2 |
| 2. SLCCI altimetry product assessment | 2 |
| 2.1. Global Mean Sea Level | 2 |
| 2.1.1. Long term trends | 4 |
| 2.1.2. Inter-annual variability | 4 |
| 2.1.3. Annual Cycle | 5 |
| 2.1.4. High Frequency Signals | 6 |
| 2.1.5. Summarizing global average performance | 6 |
| 2.2. Regional Mean Sea Level | 7 |
| 2.2.1. Long term trends | 7 |
| 2.2.2. Inter-annual signals | 8 |
| 2.2.3. Annual cycle | 8 |
| 2.2.4. High Frequency signals | 9 |
| 2.3. Local Mean Sea Level | 11 |
| 2.3.1. Long term trends | 11 |
| 2.3.2. Inter-annual variability | 12 |
| 2.3.3. Annual Cycle | 12 |
| 2.3.4. High Frequency signals | 13 |
| 3. Comparison between SLCCI and DUACS products with respect to in-situ data | 13 |
| 3.1. Global Mean Sea Level | 14 |
| 3.2. Regional mean sea level | 15 |
| 3.2.1. Long term trends | 15 |
| 4. Conclusions and recommendations | 17 |
| 5. References | 17 |
| Appendix A - List of acronyms | 19 |



1. Introduction

The purpose of this report is to present the results of the altimetry/in-situ comparisons performed within the framework of the ESA Sea Level CCI project. In-situ data are used as an external and independent source of comparison.

The first and major goal of this work is to assess and describe the consistency between two independent measurements of the physical quantity of interest: the Sea Level Anomaly (hereinafter noted SLA).

A secondary goal of this document is to attempt to demonstrate the improvements achieved by the new satellite altimetry sea level dataset generated within the project with respect to previously existing datasets.

1.1. Data description

Three types of sea level measurements are used here, satellite altimetry, tide gauge measurements and dynamic height anomalies derived from Argo temperature and salinity profiles.

Two satellite altimetry datasets are considered in this work:

- The Sea Level CCI dataset (hereinafter noted SLCCI) which was generated during the ESA Sea Level project after a careful selection of algorithms in order to achieve the highest climate-oriented performance levels. The dataset consists in weekly SLA grids spanning 18 years from 1993 to 2010,
- A dataset directly derived from the SALTO/DUACS processing but generated at the same spatial and temporal resolution than the SLCCI product to ensure consistency of the SLA estimations,
- Monthly tide gauge records are downloaded from the PSMSL database and corrected for the glacial isostatic adjustment using the ICE5G-VM4 model (Peltier, 2004) and for atmospheric effects using ERA model outputs,
- Temperature and Salinity profiles measured by Argo floats are retrieved from the Coriolis GDAC database (<http://www.coriolis.eu.org/>). For each profile, a steric Dynamic Height Anomaly (DHA) is computed using a reference level at 900 dbar and a contemporaneous mean dynamic height (also called synthetic climatology). Grace observations from the JPL are also used to constraint the mass component that is missing in the Argo observations (<http://grace.jpl.nasa.gov>; Chambers 2006). Altimeter SLA and GRACE are collocated to Argo in-situ DHA to perform the comparison. Hereinafter, the term "Argo profiles" refers to the sum of the steric height calculated from the Argo temperature and salinity measurements and mass component derived from GRACE gravity measurements.

1.2. Data comparison methods

The methodology used to compare satellite altimetry and in-situ measurements (Tide gauges and Argo profiles) is extensively described in the annual reports dedicated to these activities (reference) the interest of such comparisons is further demonstrated by Valladeau et al. (2012). Here we give only a brief overview of the methods.

1.2.1. Tide gauges

For every available station in the PSMSL database, we compute the correlation coefficients between altimetry and the tide gauges record within a 100 km radius area from the station's position. The matching satellite altimetry time series is extracted at the position of the maximum of correlation, given that:

- Correlation coefficient is higher than 0.3,



- Differences between the two records do not exceed 12 cm with standard deviation lower than 30 cm,

This procedure leads to a subset of PSMSL database with a matching altimetry time series for each tide gauge station. To limit the impact of gaps in the tide gauges series, only the tide gauge time series which are at least 80% complete (and the matching satellite altimetry time series) are considered in this work. The dataset used to estimate statistics consists in 475 pairs of tide gauges and corresponding altimetry time series.

Tide gauge time series should be commonly referenced before estimating ensemble averages. In the standard procedure the bias (estimated as the mean of the differences) between altimetry and tide gauge is removed from the tide gauge record. This method prevents any determination of regional biases between the two types of observations, but can deal with large gaps in tide gauge time series. Here, as we consider only almost complete tide gauge records, we rather removed the mean from each tide gauge time series, a method already used for global average comparisons between altimetry and tide gauges (Prandi et al., 2009).

It should be noted that the spatial sampling achieved by the tide gauges is far from even along the global ocean coasts, with a strong bias towards the northern hemisphere. The purpose of this work is not to extrapolate global average sea level from these data. When comparing to altimetry data, we apply the tide gauge spatial sampling to the altimetry data in order to perform a spatially consistent comparison.

1.2.2. Argo profiles

For each Argo profile data, the gridded satellite altimetry SLA is interpolated bilinearly at the time and position of the profile. Whenever the difference between altimeter SLA and the steric Argo dynamic height exceeds 20 cm, the data point is removed from further analysis. Satellite altimetry and in-situ SLA pairs are then used to estimate statistics on a $2^\circ \times 2^\circ$ grid with a temporal resolution of 10 days.

1.3. Description of work

This work benefits from the Round Robin Data Package (RRDP) framework developed within the Sea Level CCI project to assess the quality of two equivalent terms of the satellite altimetry equation. Following this framework, in this work, differences between in-situ and satellite altimetry estimates of SLA variability are separated into different temporal (long-term trends, inter-annual variability, annual signal, high frequency signal) and spatial (global mean, basin-wide averages, local phenomena) scales.

The major advantage of such approach is to allow an independent assessment of the agreement between satellite altimetry and in-situ measurements for the different scales of the climate signals the Sea Level CCI is dedicated to, at the cost though of a certain level of complexity.

2. SLCCI altimetry product assessment

In this section we assess the performance of the satellite altimetry SLA grids calculated within the framework of the SLCCI project by comparing them to independent measurements of the SLA by two types of in-situ probes: tide gauges and Argo floats.

The comparisons performed are classified by spatial and temporal scales of the signal considered.

2.1. Global Mean Sea Level

First we consider global average SLA as the raw result, without any post-processing, of the comparison procedure. The global average SLA time series estimated from altimetry, tide gauges



and in-situ profiles with the adequate collocation methods are presented on Figure 1. Satellite altimetry time series are represented in red while in-situ estimates are represented in blue on both graphs.

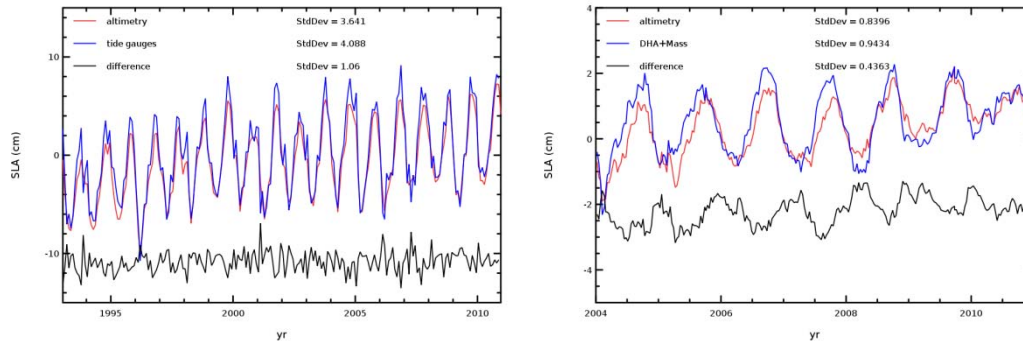


Figure 1: Time series of the global mean SLA from tide gauges and collocated altimetry (left) and from altimetry and Argo profiles (right), the differences time series are artificially translated vertically.

Regarding the global mean SLA, SLCCI and in-situ data show a good agreement:

- correlation coefficients are 0.96 and 0.84 when comparing altimetry to tide gauges and Argo profiles, respectively (correlations drop to 0.85 and 0.68 when annual and semi-annual signals are removed)
- the RMS differences are 1.2 cm and 0.6 cm when comparing altimetry to tide gauges and Argo profiles, respectively

However the time series are marked by an important annual cycle which may be masking the other temporal scales of the SLA variability. A first way to separate temporal scales is to look at the coherence between altimetry and in-situ data. Figure 2 shows the coherence between the global mean SLA time series of Figure 1. Coherence levels at low frequencies (long periods) should be viewed with caution given the relatively short time span available, and Figure 2 thus is focused on periods shorter the 900 days. The annual signal is clearly the most coherent signal between altimetry and tide gauges (wide peak around $T=365$ days). For the comparison to Argo profiles the peak is shifted towards shorter periods, probably as a result of the small phase shift between altimetry and in-situ annual signals visible on Figure 1. Coherence is also important at higher frequencies, with significant levels for the semi-annual signal, and two months signal, which is a lower limit considering monthly PSMSL tide gauges comparisons.

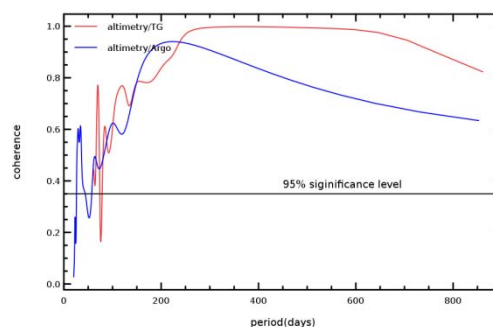


Figure 2: Coherence diagram between altimetry and tide gauges (red), and between altimetry and Argo floats (blue) for the global mean SLA time series



2.1.1. Long term trends

Considering global mean sea level, long term trend is arguably the figure which catches most attention. Table 1 summarizes the global mean sea level trend evaluated from in-situ data and collocated altimetry.

It should be noted that the SLCCI/TG comparison is performed over the whole altimetry period (1993-2010). However Argo T/S profiles are only available after 2004 and the comparison is therefore limited to the end of the period. Given the uncertainties on the comparison method (-0.7 mm.yr^{-1} for the tide gauge comparison and $\sim 1 \text{ mm/yr}$ for the Argo profiles comparison) between altimetry and in-situ data, there is almost no drift of the altimetry with respect to tide gauges. However, Argo profiles see a slightly lower sea level rise than the altimetry.

| | Tide gauges (1993-2010) | Argo profiles (2004-2010) |
|------------|-------------------------|---------------------------|
| Altimetry | 2.9 | 2.0 |
| In-Situ | 2.7 | 0.9 |
| difference | 0.2 | 1.1 |

Table 1 : Global Mean Sea Level trends evaluated from altimetry data and in-situ measurements (all trends are expressed in mm.yr^{-1})

2.1.2. Inter-annual variability

The inter-annual variability considered here corresponds to signals with periods larger than two years but without the long-term trends. Despite its low amplitude (compared to the annual signal for example), this frequency domain of the SLA signal variability is of climatic importance, as it depends on low-frequency oscillations of the climate system.

To obtain the inter-annual time series, we apply a low-pass filter to the detrended time series of Figure 1, in order to remove all signals with periods lower than two years. The time series of the global mean SLA inter-annual variability are displayed on Figure 3, for the tide gauge and Argo profiles comparison.

For the altimetry/tide-gauges comparison however, there is a very good agreement between in-situ and altimetry records, both for the amplitude and the phasing of the inter-annual variability, as suggested by the coherence diagram of Figure 2. The correlation between the time series of Figure 3 is very high at 0.94, but tide gauges still record a higher level than the altimetry does.

It should be noted that for the Argo comparison, the inter-annual variability is small with about 0.5 cm maximum amplitude. The short period available (only 7 years) is an important limit for this type of low-frequency signals comparison, and uncertainty levels are high. If the two time series show a consistent behavior ($r=0.68$), there appears to be a shift in the phasing of the signals, resulting in a standard deviation of the differences almost as large as the altimetry or Argo time series. The satellite altimetry time series displays a larger inter-annual variability levels than the Argo time series.

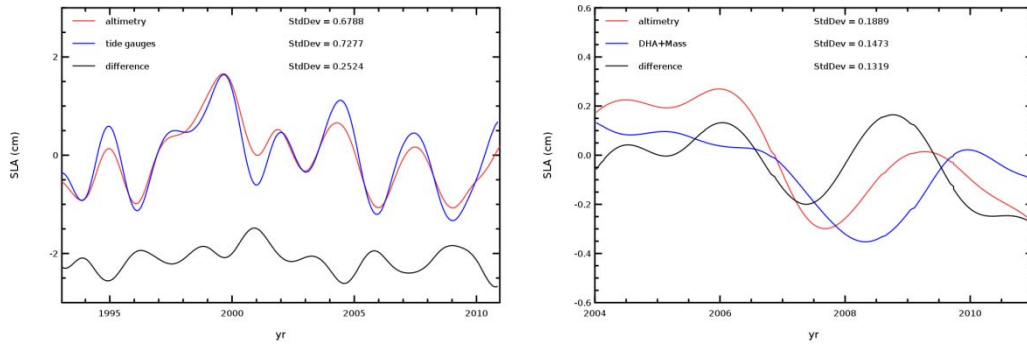


Figure 3: Time series of the inter-annual variability of the global mean SLA from tide gauges (left) and Argo profiles (right), and the corresponding co-located altimetry.

Regarding global average inter-annual variability, the comparison to tide gauges records shows that the SLCCI altimetry dataset performs well in reproducing the observed sea level variability. Performance is somewhat lower when comparing it to Argo profiles but given the short period available, inter-annual signals should be viewed with caution.

2.1.3. Annual Cycle

From Figure 1, it is apparent that the annual cycle explains an important part of the variability of the global mean SLA, either observed by satellite altimetry or by in-situ data. The seasonal cycles derived from the time series of Figure 1 are represented on Figure 4.

Considering the altimetry/tide gauges comparison, there is an excellent agreement between annual cycles, both in term of amplitudes (altimetry amplitude is about 1 cm lower than the tide gauges one) and phasing of the signal (the minimum is reached in March while the maximum is reached in September for both datasets).

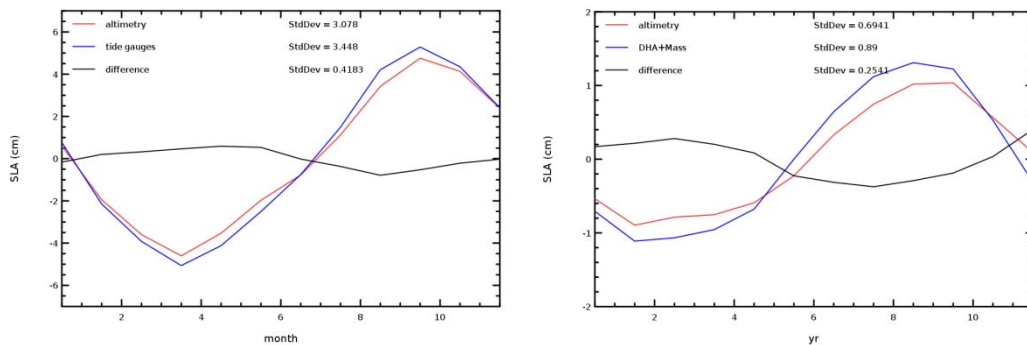


Figure 4: Global mean SLA annual cycle estimated from tide gauges and Argo T/S data, and the corresponding co-located satellite altimetry (95% confidence levels for the monthly mean are overlaid as thin grey lines for the in-situ estimates)

When comparing altimetry to Argo profiles, the altimetry amplitude is lower than the Argo one, and the two seasonal cycles seem shifted by one month (altimetry being delayed) for the position of the maximum. It should however be noted that the amplitude of the seasonal cycle measured by Argo is much lower than the one measured by tide gauges, one possible cause for this is that, as Argo samples a much broader part of the ocean than tide gauges, out of phase signals in the Northern and Southern hemispheres are averaged out.

On a global scale, the SLCCI satellite altimetry dataset is in very good agreement with in-situ data regarding the seasonal cycle, which is an important part of the total SLA variability.



2.1.4. High Frequency Signals

The previous sections of this report were dedicated to long-term trends, inter-annual variability and the seasonal cycle. After these signals have been removed from the total SLA time series, only the high-frequency variability remains. Figure 5 shows the high frequency variability of the global average SLA time series of in-situ and collocated satellite altimetry. Here we consider signals with a period shorter than six months.

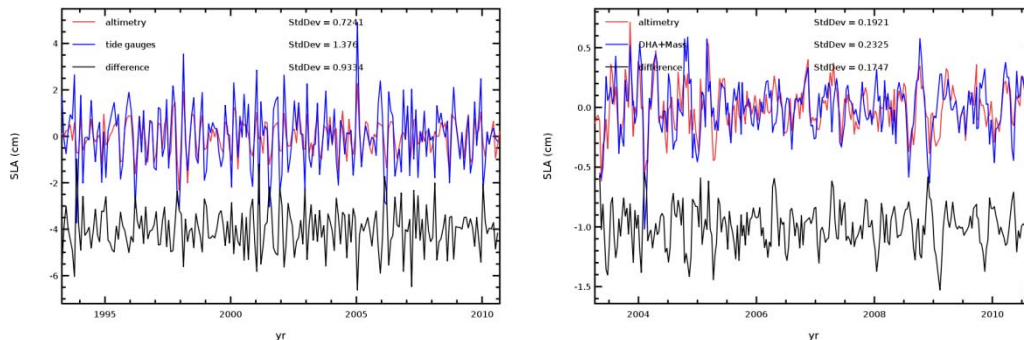


Figure 5: Time series of the high frequencies of the SLA from tide gauges (left) and Argo profiles (right), and the corresponding co-located altimetry. The time series of the differences are represented in black with an artificial vertical shift.

The high frequencies represent an important part of the total SLA variability with standard deviations of 1.4 cm and 0.7 cm for the tide gauge and collocated altimetry data (standard deviations are 4.1 cm and 3.6 cm for the total SLA content (high and low frequencies)) for example. For both comparisons, correlations are high between altimetry and in-situ ($r=0.78$ for tide gauges and $r=0.68$ for Argo profiles), though satellite altimetry records show lower levels of high frequency variability than in-situ records, and the standard deviation of the differences has the same magnitude than altimetry or in-situ records alone.

2.1.5. Summarizing global average performance

In order to provide a synthetic look on the comparisons between global mean SLA estimated from altimetry and in-situ data for the different temporal scales considered in this study, Figure 6 displays a Taylor diagram summarizing these different aspects. In this figure, all standard deviations are normalized by the corresponding altimetry standard deviation for convenience purposes, and the RMS of the difference therefore can't be read directly from the graph.

For the altimetry/tide gauges comparison, the annual and inter-annual signals are in very good agreement with correlations higher than 0.9 and comparable variability levels resulting in low RMS of the differences (0.58 and 0.24 cm respectively). The performance is much lower for the high frequency part of the signal, due to very difference standard deviations.

It is interesting to note that generally, the performance of the Argo profiles comparison is slightly lower, regardless of the period of the signal considered except for the high frequencies of the signal. For inter-annual variability, the correlation between altimetry and Argo profiles is low ($r=0.68$, red dot on Figure 6) resulting in a high RMS difference, even if the two techniques show comparable variability levels.

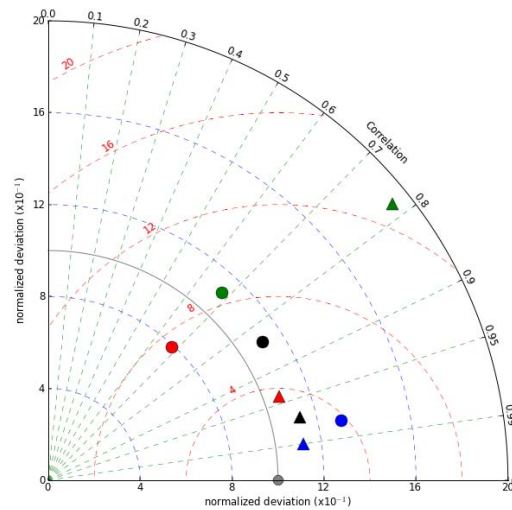


Figure 6: Taylor diagram comparing altimetry (grey dot), tide gauges (triangles) and Argo profiles (circles) for the raw signal (black), the inter-annual signal (red) and the annual cycle (blue) and the high frequencies of the SLA (green)

For both the altimetry/tide gauges and altimetry/Argo profiles comparisons, the seasonal cycle, which is a dominant signal in the global average variability, is in good agreement between altimetry and in-situ data.

2.2. Regional Mean Sea Level

After considering the global mean SLA, in this section we consider smaller spatial scales and investigate the comparison between altimetry and in-situ for basin-wide averages. When moving from global average to basin-wide (or regional) average the SLA variability should increase, at least in some areas. In this study we consider three major ocean basins: the Pacific, Atlantic and Indian Oceans. As in the previous section, the SLA variability is separated by time scales.

2.2.1. Long term trends

The basin average SLA trends, estimated from in-situ data and co-located SLCCI altimetry, are summarized in Table 2.

| | | Pacific Ocean | Atlantic Ocean | Indian Ocean |
|-----------|---------------|---------------|----------------|--------------|
| 1993-2010 | altimetry | 2.1 | 2.7 | 4.0 |
| | tide gauges | 1.7 | 2.1 | 4.2 |
| | difference | 0.4 | 0.6 | -0.2 |
| 2004-2010 | altimetry | 0.6 | 2.1 | 5.1 |
| | Argo profiles | 0.0 | 0.4 | 4.4 |
| | difference | 0.6 | 1.7 | 0.7 |

Table 2: SLA trend differences (mm/yr) between altimetry and in-situ estimated over different oceanic basins

For the altimetry/tide gauges comparisons, trend differences are evenly distributed for the three oceanic domains considered in this study. The largest trend difference is observed in the Atlantic



Ocean with 0.6 mm.yr^{-1} drift between the two techniques. Such a difference is below the uncertainty of the method (-0.7 mm.yr^{-1} for the global average, and certainly higher for a regional average) and therefore not significant. The Indian Ocean is poorly sampled and uncertainties are much larger in this area, despite the good agreement between the two techniques.

Trend differences are larger for the altimetry/Argo profiles comparison, and all positive, reflecting a larger and spatially consistent global mean drift of the SLCCI altimetry dataset compared to Argo floats, altimetry always measuring a higher rate of sea level rise than Argo floats. The largest trend difference is again observed in the Atlantic Ocean with a 1.7 mm/yr trend difference, larger than the methodology uncertainty.

2.2.2. Inter-annual signals

In order to summarize the inter-annual variability comparisons for basin-wide SLA averages, the corresponding Taylor diagram is represented on Figure 7.

High values of the correlation coefficients are found for the altimetry/tide gauges comparisons over all three oceans ($r > 0.75$), but with higher levels of variability for the tide gauge records than the altimetry. Such feature is observed on all temporal and spatial scales. Performances of the altimetry versus tide gauge are fairly similar in the Atlantic and Pacific Oceans.

Regarding the comparison to Argo floats, and unlike the comparison to tide gauges, the different basins show different behaviors. In the Pacific and Atlantic Oceans, the altimetry variability is higher than the in-situ one. The opposite is observed in the Indian Ocean.

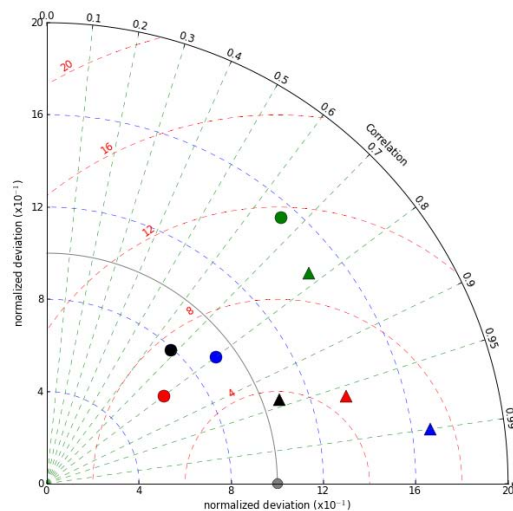


Figure 7: Taylor diagram comparing tide gauges (triangles) and Argo profiles (circles) for the inter-annual signal of the ocean-basin wide averages of SLA over the Pacific Ocean (red), the Atlantic Ocean (blue) and the Indian Ocean (green). The global mean is represented in black

For both the altimetry/tide gauges and altimetry/Argo profiles comparison, the performance is lower in the Indian Ocean than in other basins, but with a consistent behavior of both tide gauges and Argo comparisons. The low tide gauge sampling along the coasts of the basin might explain part of the observed differences, but more investigations are required regarding the altimetry/Argo comparison.

2.2.3. Annual cycle

For the global mean SLA, annual cycles estimated from in-situ records and collocated SLCCI altimetry show a good agreement, despite the one month shift observed between Argo profiles and collocated altimetry.



Figure 8 displays the SLA seasonal cycle estimated from tide gauge and collocated altimetry records over the Pacific, Atlantic and Indian oceans. Over the three basins considered, the SLCCI altimetry dataset observes a seasonal cycle very close to the one observed by tide gauges.

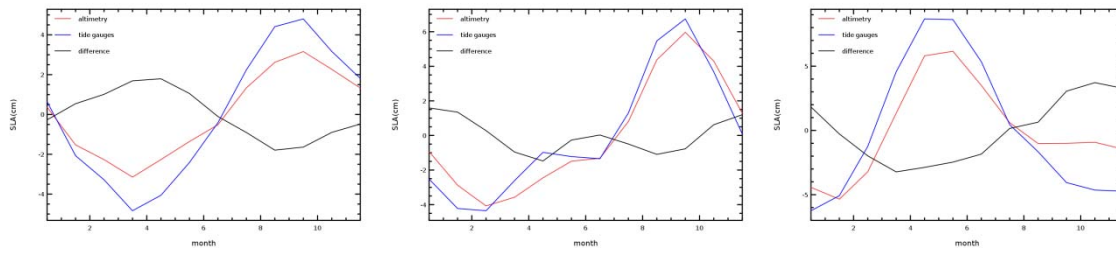


Figure 8: Basin-wide average SLA annual cycle for altimetry and tide gauge data for the Pacific Ocean (left), the Atlantic Ocean (center) and the Indian Ocean (right)

Figure 9 is similar to Figure 8 but for the SLA derived from Argo profiles and collocated altimetry. The seasonal cycles in the Pacific and Atlantic Oceans observed by Argo profiles and collocated altimetry are very similar: amplitudes differences are small and there is no phase shift. The agreement is much poorer in the Indian Ocean where seasonal cycles observed by the two techniques are very different, both in term of amplitude and phase.

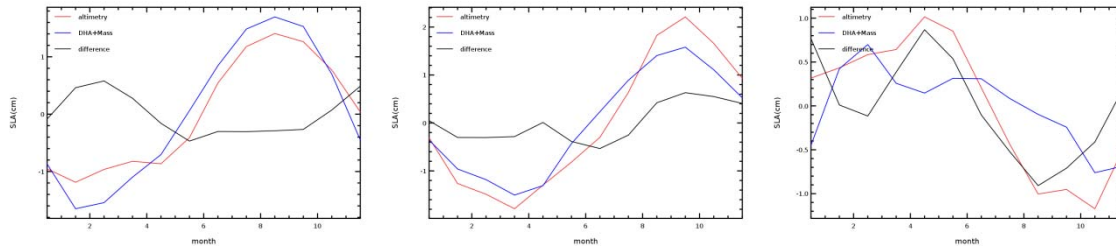


Figure 9: Basin-wide average SLA annual cycle for altimetry and Argo data for the Pacific Ocean (left), the Atlantic Ocean (center) and the Indian Ocean (right)

2.2.4. High Frequency signals

The performance of in-situ records with respect to collocated altimetry regarding the high frequency part of the regional average SLA over the Pacific, Atlantic and Indian Oceans is summarized on the Taylor diagram of Figure 10.

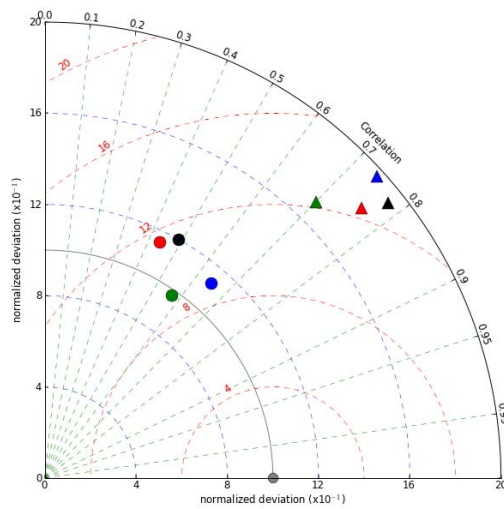


Figure 10: Taylor diagram comparing tide gauges (triangles) and Argo profiles (circles) for the high frequencies of the basin-wide mean SLA over the Pacific Ocean (black), the Atlantic Ocean (red) and the Indian Ocean (blue)

At this spatial and temporal scale of the SLA signal, some of the features already observed still hold true: tide gauges SLA variability is higher than collocated altimetry SLA variability, although correlations remain high ($r > 0.7$). The high frequency variability of the Argo profiles' SLA is close to the collocated altimetry one, but correlations are generally lower than for the comparison to tide gauges. For both in-situ data comparisons, the three basin averages considered display similar performances with respect to altimetry data.

Figure 10 does not separate the different scales present in the high frequencies of the signal as we consider them here. In order to investigate those smaller scales, we calculate the coherence diagram between the high frequencies of the basin-wide average SLA estimated from in-situ records and co-located altimetry. The corresponding coherence diagrams are presented on Figure 11. The monthly sampling of the tide gauge data limits the resolution achievable by the analysis. The comparison between altimetry and Argo profiles is performed with a ten day temporal sampling so higher frequency behaviours are observable: coherence values are high for very short periods (20-30 days), and again around 70 days, especially in the Indian and Atlantic Oceans. In the Indian Ocean, coherence around a one year period is lower than in other basins, in agreement with larger seasonal cycle differences between altimetry and in-situ in this basin than in the others.

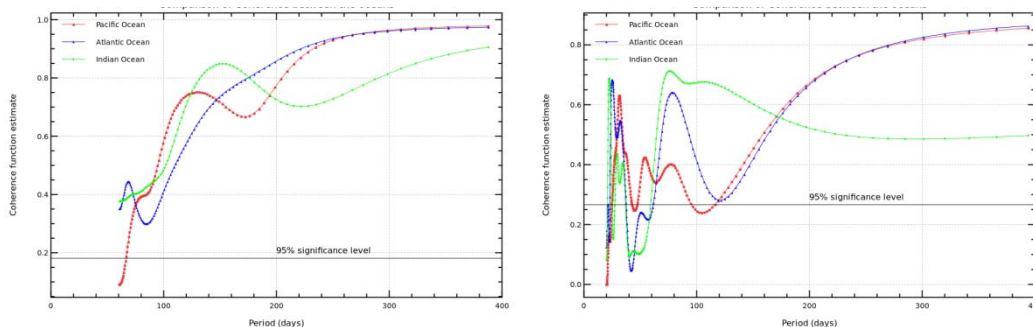


Figure 11: Coherence diagram between tide gauges and co-located altimetry (left) and Argo profiles and co-located altimetry (right) data for the high frequencies of the Pacific (red), Atlantic (blue) and Indian (green) oceans



2.3. Local Mean Sea Level

In this section, in order to get a hint of the spatial distribution of the differences between altimetry and in-situ records, we map these differences after separating the total SLA signal into temporal scales. When considering local averages (2° box average for the Argo comparison and individual time series for the tide gauge comparison), uncertainties are much larger than when considering the global average and therefore estimates of the differences should be viewed with caution.

2.3.1. Long term trends

First we investigate long term trends. The maps of trend differences between in-situ records and collocated SLCCI satellite altimetry are displayed on Figure 12. The left panel referring to the altimetry/tide gauges comparison shows the spatial distribution of the stations used in this study. Some regions seem to have coherent drifts: along the coast of Norway or in the north-western Atlantic Ocean for example. This could indicate an error in the altimetry data, or in tide gauges data (for example subsidence of the earth's crust that would affect all tide gauges stations in a region). The Argo profiles/altimetry comparison maps shows trends that seem evenly spatially distributed, no large coherent spatial patterns are found.

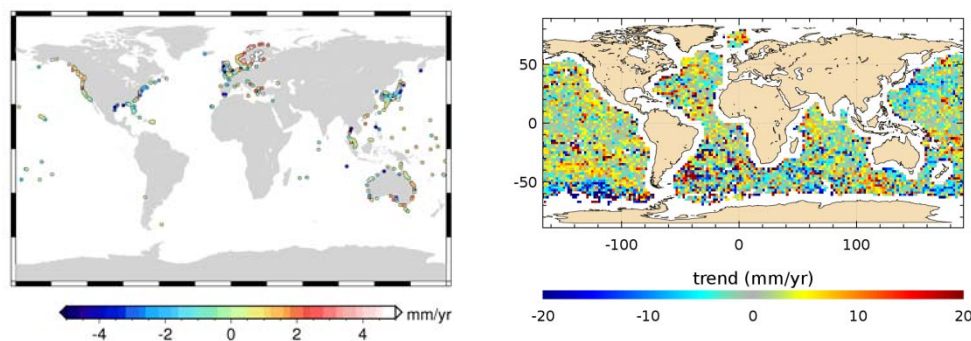


Figure 12: Map of the SLA differences trends between altimetry and tide gauges (left) and between altimetry and Argo profiles (right)

For both the tide gauges/altimetry and Argo profiles/altimetry comparisons, the low drifts observed when considering global or basin-wide averages appear on the map of Figure 12 to hide a wide distribution of the individual stations' trends.

The distribution of the trend differences between altimetry and in-situ records is further investigated by the means of the histograms displayed on Figure 13, illustrating the wide spread of the trend differences.

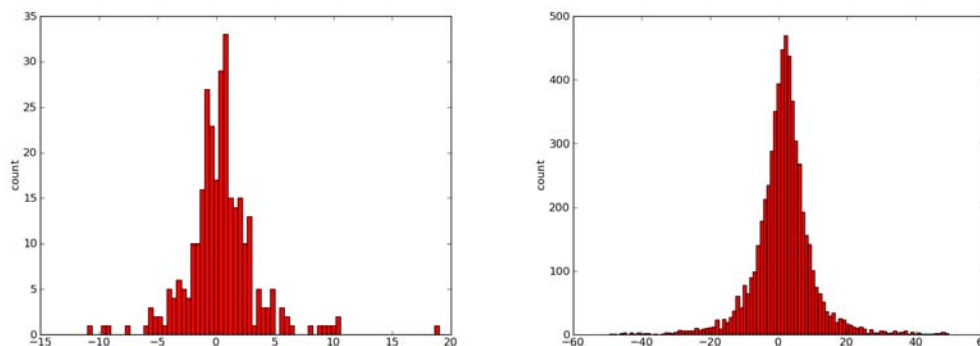


Figure 13: Histograms of the trend differences (in mm/yr) between tide gauges and co-located altimetry (left) and Argo profiles and co-located altimetry (right)



2.3.2. Inter-annual variability

Figure 14 displays the maps of SLA variance differences between altimetry and in-situ data estimated from the low-frequency (i.e. inter-annual variability) of the signal.

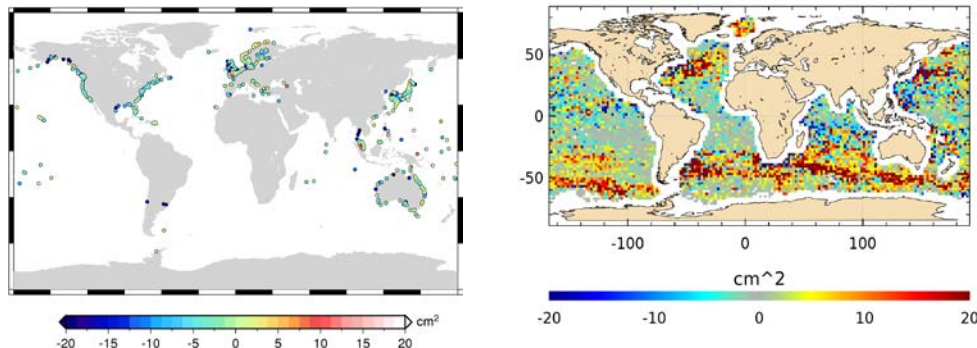


Figure 14: Map of the inter-annual SLA variance differences between altimetry and tide gauges (left) and between altimetry and Argo profiles (right)

On the comparison between SLCCI altimetry dataset and Argo profiles (right panel) high oceanic variability areas (ACC, western boundary currents) stand out with positive values, meaning that in these areas, altimetry records observe higher SLA variances than the Argo profiles.

The SLCCI altimetry/tide gauges comparison shows a good performance, with most of the variance differences ranging between -5 and 5 cm^2 despite some extreme values.

2.3.3. Annual Cycle

As was demonstrated on global or regional averages, the annual cycle is an important part of the total SLA variability, especially when considering the comparison between altimetry and tide gauges. When considering global or basin-wide averages, there is generally a good agreement between altimetry and in-situ data (excepted in the Indian Ocean). In order to investigate the spatial distribution of the annual signal differences, we computed maps of the annual signals differences between altimetry and in-situ records.

Figure 15 represents the spatial distribution of annual cycle amplitude and phase differences between tide gauge and collocated satellite altimetry data. Phase differences appear to be evenly distributed with low differences (15 degrees represents half a month shift in the phasing of the annual cycle) observed at all stations. The map of amplitudes differences displays a different behavior: differences are low in the Atlantic Ocean but much higher for the coastal stations of the Pacific Ocean (differences remain low for island stations).

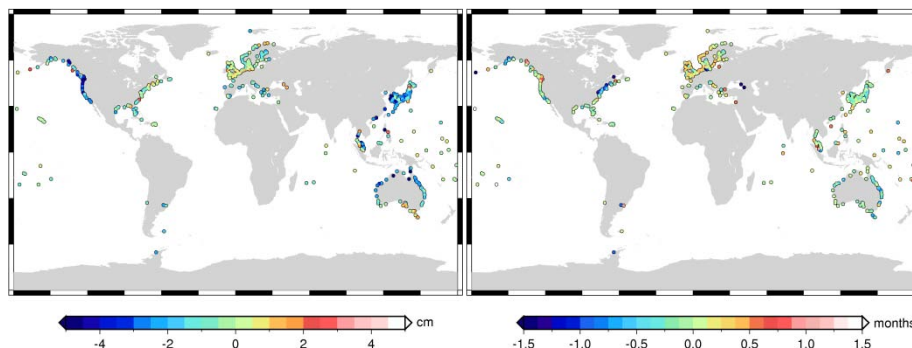


Figure 15: Maps of the annual cycle amplitude (left) and phase (right) differences between SLCCI altimetry and tide gauges

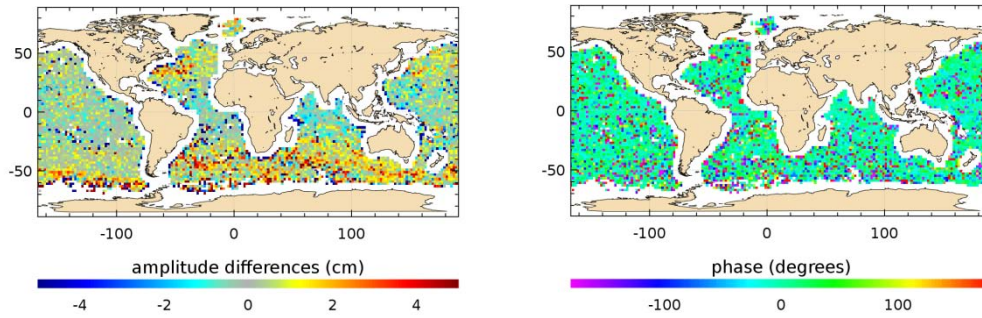


Figure 16: Maps of the annual cycle amplitude (left) and phase (right) differences between SLCCI altimetry and Argo profiles

Figure 16 shows the maps of the differences between altimetry and Argo profiles for the amplitude and phase of the annual signal. The phase differences appear to be very noisy but with an evenly distributed spatial pattern. The map of the amplitudes differences displays a latitude dependant pattern with negative differences in the tropical band where Argo profiles are seeing a larger amplitude than the altimetry and positive differences at lower latitudes (especially in the southern hemisphere) where altimetry amplitudes are larger than Argo ones. Again, in high oceanic variability areas such as the Gulf Stream, the differences are large.

2.3.4. High Frequency signals

The maps on Figure 16 display the variance differences between altimetry and in-situ collocated records for the high frequency part of the SLA variability. Tide gauges stations generally observe higher variability levels for this frequency band than the corresponding altimetry. However, island stations seem to show a better agreement with altimetry than continental coastal ones.

The altimetry versus Argo profiles comparison map displays a latitude dependant pattern: in the tropical band of all oceanic basins, variance differences are negative indicating higher variability levels in the in-situ records than in the altimetry data. In areas of high oceanic variability (ACC, Gulf Stream and Kuroshio) variability levels measured by Argo floats are lower than the altimetry ones.

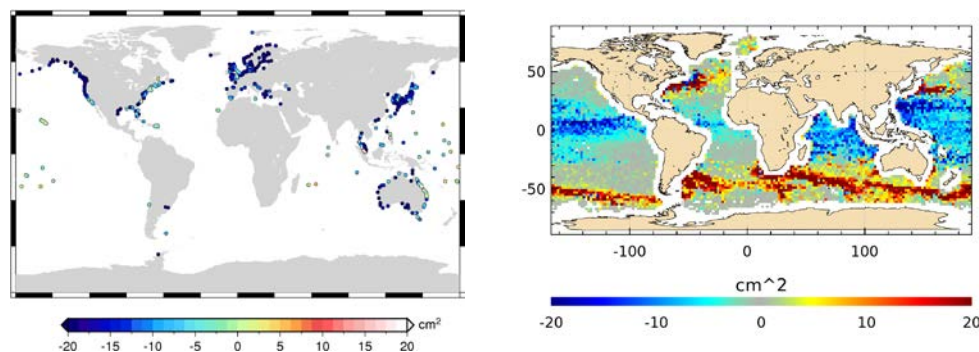


Figure 17: Map of the differences of SLA variances between altimetry and tide gauges records (left) and between altimetry and Argo profiles (right) for the high frequency part of the signal

3. Comparison between SLCCI and DUACS products with respect to in-situ data

The previous section of this report was dedicated to the comparison of the satellite altimetry SLA gridded dataset generated within the SLCCI project. One secondary objective of the study,



presented in this section, is to compare two satellite altimetry products with respect to available in-situ data (both tide gauges and Argo profiles).

For this purpose, we considered the SLCCI dataset and compared it to a reference dataset based on SALTO/DUACS processing, adapted to match the monthly temporal resolution of the SLCCI grids. Different spatial and temporal scales of the signal are studied, with the objective of determining which dataset fits the in-situ data (considered here as the "truth") best.

The spatial and temporal scales of the signal at which comparisons with in-situ data are investigated depend on a first evaluation of the differences between the two altimetry datasets. We focused on scales where the largest differences between the two altimetry datasets were found.

3.1. Global Mean Sea Level

When considering SLA time series averaged globally, the differences between the two datasets are very small. As an example, Figure 17 displays the global mean SLA time series estimated from the SLCCI and SALTO/DUACS datasets. Apart from years 1994 and 1995, the differences between the two time series are very low. As a result, the long term trends differ only by 0.02 mm/yr, a value which is not statistically significant (Ablain et al, 2009 estimated that the uncertainty on the global mean sea level trend is about 0.5 mm/yr). The same results are found for the other temporal scales of the global mean SLA considered in this study (inter-annual, seasonal and high-frequency variability).

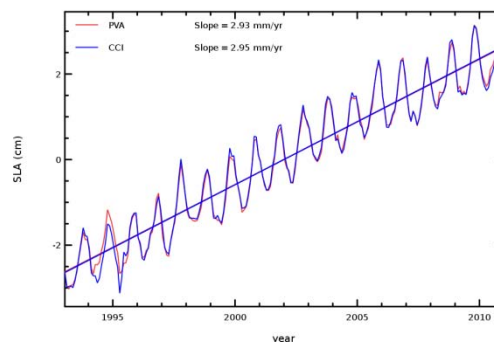


Figure 18: Time series of the global mean SLA estimated from the SLCCI (blue) and PVA (red) satellite altimetry datasets

Given the uncertainty levels of the altimetry/in-situ comparison method (about 0.5 mm/yr for the global mean SLA trend for example) it is hard to discriminate the two altimetry products when considering global averages. However, Figure 19 displays the differences observed between altimetry and in-situ for the different temporal scales of the global average signal for both the CCI/in-situ and DUACS/in-situ comparisons. For almost all time scales considered here, the in-situ data seems to be closer to the CCI data (triangles) than the DUACS data (circles). This results suggests that there is a better agreement between CCI altimetry and in-situ data than between DUACS altimetry and in-situ.

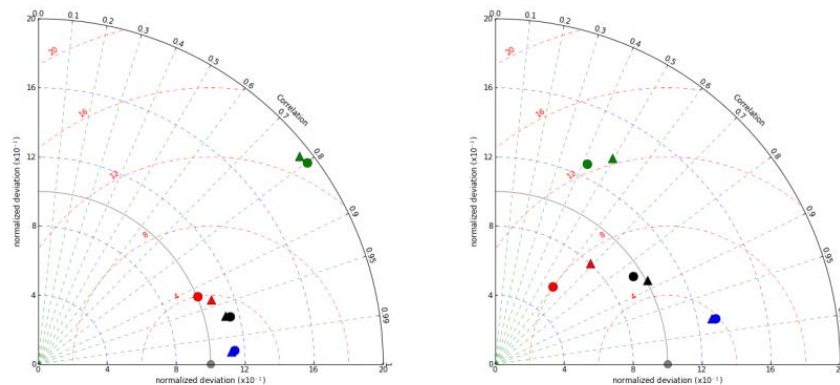


Figure 19: Taylor diagrams comparing altimetry and in-situ data (left: tide gauges, right: Argo profiles) for CCI (triangles) and DUACS (circles) data. Global averages are considered for the total signal (black), the annual cycle (blue), the inter-annual variability (red) and the high frequencies (green)

3.2. Regional mean sea level

We showed that differences between satellite altimetry datasets were too low on the global average to be separated by the comparison to in-situ data. When moving from global to regional averages, and depending on the region used to calculate spatial averages, one can expect the differences between the two satellite altimetry datasets to become larger, and therefore to be able to discriminate those two datasets by means of the comparison to in-situ data.

Of course what “regional” means may well vary, and choosing the suitable region for averaging results from a compromise: the smaller the averaging region, the larger the differences at the cost of increased noise and errors. In this study, we considered large regional averages, typically basin-wide.

3.2.1. Long term trends

Figure 18 displays the maps of SLA trend differences between SLCCI and SALTO/DUACS altimetry datasets for the whole altimetry period and for the last part of the period, over which Argo profiles are available. The very low difference observed on global means appears to be unevenly distributed over the globe and large areas are experiencing trend differences larger than 1 mm/yr.

Over the longest period, the trend differences map exhibits a North/South hemispheric pattern, over the Argo period; there remains a hemispheric pattern in the trend differences, but with an East/West spatial repartition. Differences are larger over the Argo period and we therefore focus on this time span (i.e. 2003.5-2010). We consider East/West hemispheric averages, for latitudes between 66°S and 66°N (thus excluding the very large trend differences observed in the Arctic Ocean).

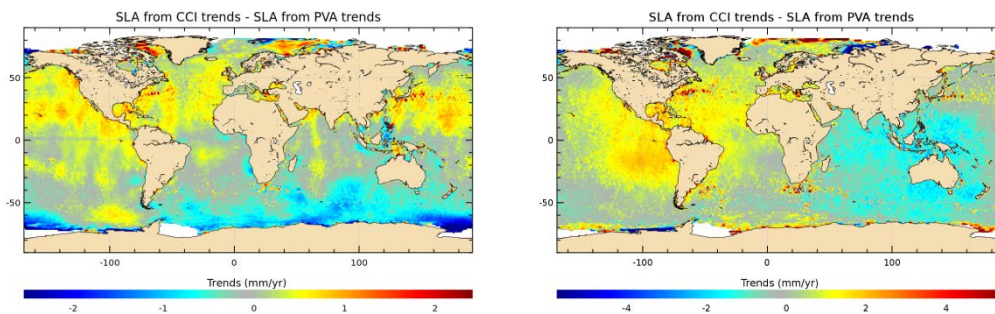


Figure 20: Maps of the SLA trend differences between CCI and SALTO/DUACS datasets, estimated over the 1993-2010 (left) and 2003.5-2010 (right) periods

The map of the drift differences between CCI and SALTO/DUACS satellite altimetry products with respect to Argo profiles (i.e. $(T_{CCI} - T_{Argo}) - (T_{PVA} - T_{Argo})$) is presented on Figure 21. This figure displays a hemispheric pattern somewhat similar to Figure 20's one, demonstrating that despite the spatial and temporal sub-sampling inherent to the altimetry/Argo comparison the technique is able to observe such trend differences.

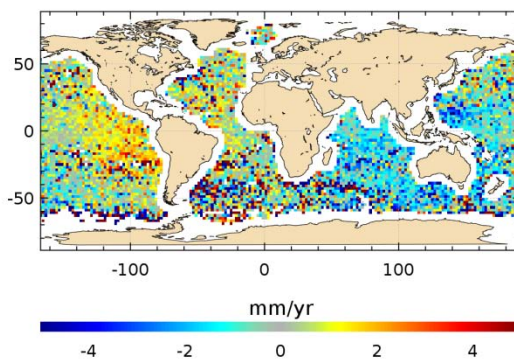


Figure 21: Map differences between trend differences between altimetry and Argo profiles evaluated with CCI and SALTO/DUACS altimetry datasets

Once the drift differences map of Figure 21 has been evaluated, there remains to investigate if the comparison to Argo profiles is useful to find the "best" altimetry dataset. We estimate East/West hemispheric SLA time series from Argo profiles, collocated SSALTO/DUACS altimetry, and collocated SLCCI altimetry. The corresponding time series are displayed on Figure 22, with the annual and semi-annual signals removed.

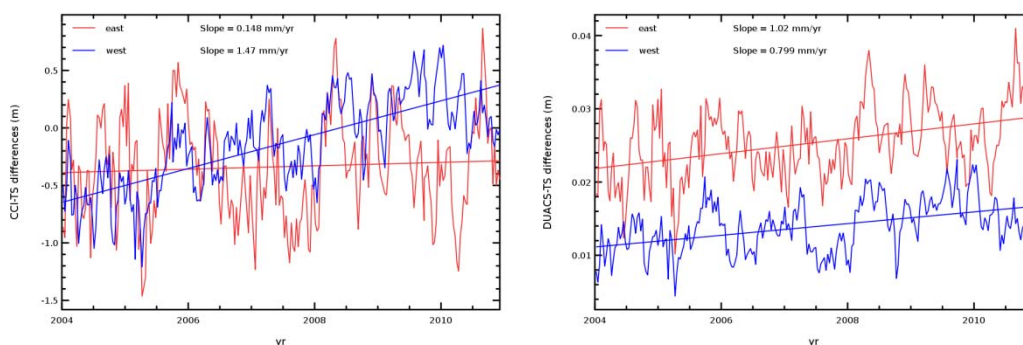


Figure 22: Time series of hemispheric SLA (west blue and east red) from Argo profiles and collocated altimetry from CCI (left) and SALTO/DUACS (right)

For the DUACS altimetry dataset, the drift respective to Argo floats is almost the same in both hemispheres. This situation is changed when considering CCI altimetry where the east/west drift



difference amounts to 1.3 mm/yr. This is expected due to the use of GDR-D orbits in the CCI products versus GDR-C orbits in DUACS. This standard change has demonstrated its relevance on Envisat data, which does not appear here because the generation process of SLCCI (and DUACS) data includes an empirical orbit error reduction step to fit Envisat data on Jason-1 over the period considered here.

4. Conclusions and recommendations

The main goal of this report was to compare the SLCCI altimetry dataset to in-situ records. Satellite altimetry was compared to two independent in-situ datasets: monthly tide gauge records from the PSMSL database and in-situ SLA derived from the combination of Argo temperature and salinity profiles and GRACE gravity data. In order to investigate the agreement between SLCCI satellite altimetry and in-situ data the different temporal and spatial scales of the SLA variability were separated: long-term trends, inter-annual variability, seasonal cycles and high-frequency variability are considered for global and basin-wide averages as well as local comparisons.

In general, tide gauge records observe higher level of variability than the collocated altimetry data, on the contrary, SLA records derived from Argo profiles and GRACE ocean mass show lower levels of variability than satellite altimetry.

The seasonal cycle is dominating the SLA variability, for both in-situ datasets and the corresponding collocated satellite altimetry. On global and regional scales, seasonal cycles agree well between in-situ and satellite altimetry records. The agreement is slightly better for the tide gauge/altimetry comparison than for the Argo profiles/altimetry one. However, these low regional differences hide a large dispersion when considering local comparisons (station or grid point wise).

The long term evolution of sea level is a main interest in climate studies. Comparing long term trends estimated over 18 years of tide gauge and collocated satellite altimetry data, we found a difference between the two techniques of only 0.2 mm/yr, and therefore a good agreement between the two records. Argo profiles are not available over the whole period, and the trend difference over the 2004-2009 period with respect to collocated satellite altimetry is higher at 1.1 mm/yr. It should be noted that this trend is heavily dependent on the GRACE mass fields used to estimate the ocean mass component added to the steric sea level estimated from the Argo temperature and salinity profiles.

A secondary goal of this report was to use in-situ data to compare the quality of two satellite altimetry datasets: the SLCCI and SALTO/DUACS grids. For this purpose we first evaluated the differences between the two satellite altimetry datasets, looking for signals large enough which could be separated by the in-situ comparison. The differences are low but suggest a better agreement to in-situ data when using SLCCI dataset rather than SALTO/DUACS. The east/west difference observed when comparing to Argo floats is expected due to the orbit changes.

5. References

Ablain, M., A. Cazenave, G. Valladeau, and S. Guinehut, 2009: A New Assessment of the error budget of global mean sea level rate estimated by satellite altimetry over 1993-2008, *Ocean Sci.*, 5:193-201.

Chambers, D.P., 2006: Evaluation of New GRACE Time-Variable Gravity Data over the Ocean. *Geophys. Res. Lett.*, 33(17), L17603.

Legouis J.F., Ablain M. 2012: CalVal altimetry / Argo annual report. Validation of altimeter data by comparison with in-situ T/S Argo profiles. Ref. CLS/DOS/NT/12-261.

Peltier, W.R., 2004: Global Glacial Isostasy and the Surface of the Ice-Age Earth: The ICE-5G (VM2) Model and GRACE, *Annual Review of Earth and Planetary Science*, 32, 111-149, 2004



Prandi, P., A. Cazenave, and M. Becker, 2009: Is coastal mean sea level rising faster than the global mean? A comparison between tide gauges and satellite altimetry over 1993–2007, *Geophys. Res. Lett.*, 36, L05602, doi:10.1029/2008GL036564.

Valladeau, G., J.-F. Legeais, M. Ablain, S. Guinehut and N. Picot, 2012, Comparing Altimetry with Tide Gauges and Argo Profiling Floats for Data Quality Assessment and Mean Sea Level Studies, *Marine Geodesy*, 35, supp. 1, pp.42-60



Appendix A - List of acronyms

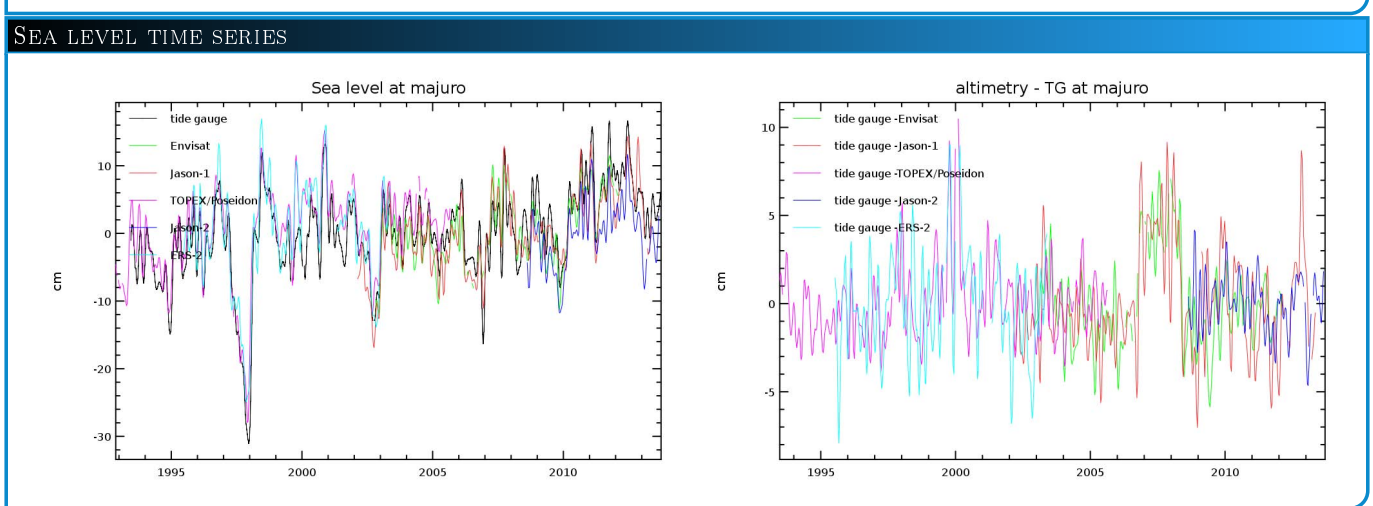
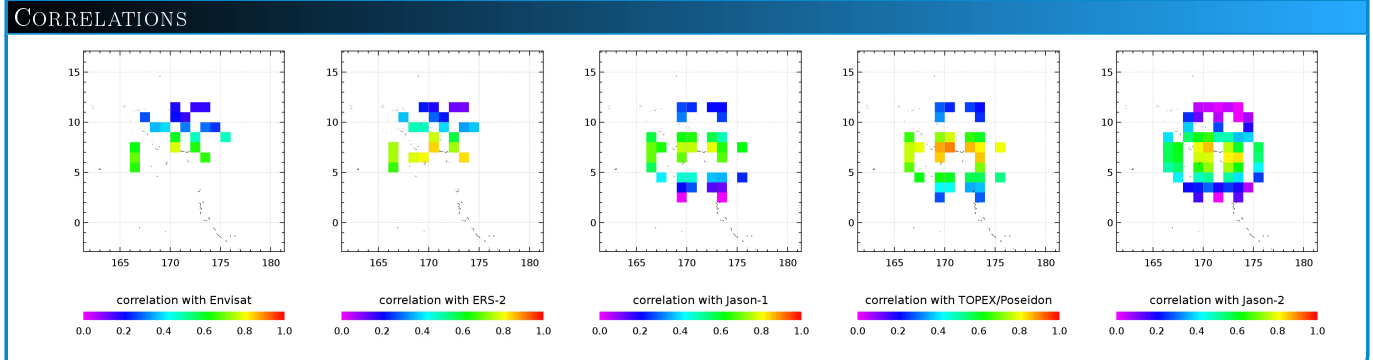
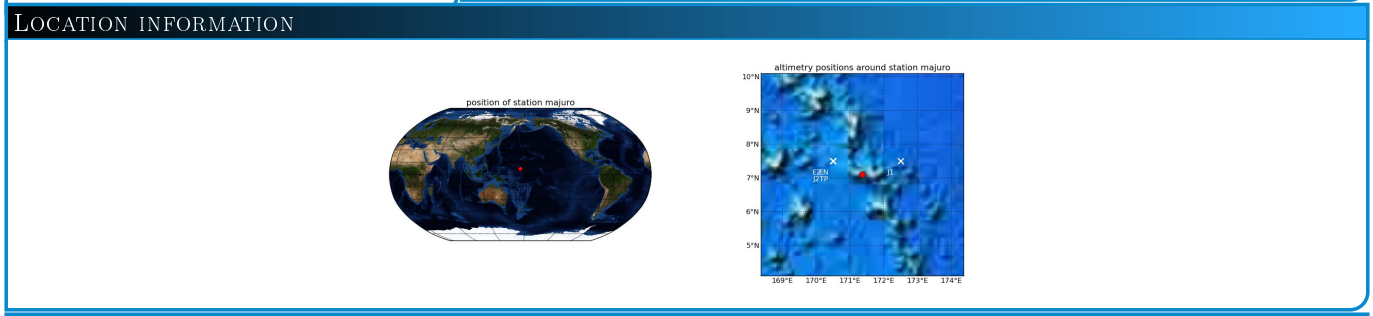
| | |
|-----|---------------------|
| TBC | To be confirmed |
| TBD | To be defined |
| AD | Applicable Document |
| RD | Reference Document |

10.3. Annex: New design of simplified in-situ information cards

COMPARISONS BETWEEN ALTIMETRY AND TIDE GAUGE DATA AT STATION MAJURO

generated on Wednesday 18th December, 2013 at 18:26:15

| GENERAL INFORMATION | | STATISTICS | | | | | |
|-----------------------------|------------|--|---------|---------|----------------|---------|--------|
| station name | majuro | statistics | Envisat | Jason-1 | TOPEX/Poseidon | Jason-2 | ERS-2 |
| station code | GC0005 | distance (km) | 105.49 | 132.76 | 105.49 | 105.49 | 105.49 |
| network name | WOCE | correlation | 0.79 | 0.80 | 0.91 | 0.86 | 0.85 |
| station latitude | 7.1 | altimeter std (cm) | 6.49 | 6.91 | 7.80 | 5.93 | 9.57 |
| station longitude | 171.366666 | tide gauge std (cm) | 6.15 | 6.28 | 7.53 | 5.76 | 8.50 |
| matching altimeter missions | 5 | rms of the differences (cm) | 4.01 | 4.16 | 3.29 | 3.07 | 5.11 |
| | | sea level drift (mm.yr ⁻¹) | -0.25 | 1.08 | 0.91 | -1.81 | 0.50 |



10.4. Annex: Global quality assessment of updated GeoSat dataset

Global Quality Assessment of updated GEOSAT Dataset

V.Koch¹, S.Philippis¹, M.Ablain¹

¹CLS, Space Oceanography Division, Toulouse, France

Overview : The U.S. Navy GEOSAT altimetric mission was the first mission to provide global data over a long period (from 1985 to early 1990). During the first 18 months, Geosat was on a geodetic orbit, afterwards it was on a 17-day exact repeat track. The last official Geosat data was released in 1997 (http://ibis.grdl.noaa.gov/SAT/gdrs/geosat_handbook/). Even though the dataset is less precise than recent altimeter datasets such as Jason-2, the Geosat data are interesting as they are the only available global altimeter data before the 1990's. Furthermore, over the years new geophysical standards (ionospheric model, wet and dry tropospheric correction from models, ...) have been available. A recent release of precise orbit ephemeris from the National Aeronautics and Space Administration is also available (GSFC 0905). In addition, the geodetic phase was retracked and is available as "20th Anniversary GEOSAT Geodetic Mission Product" (Lillibrige et al. 2006). Hereafter, the Geosat 1-Hz dataset from the RADS database (<http://rads.tudelft.nl/rads/rads.shtml>) has been used which contains already the updated standards. The quality of the updated data set is analyzed and compared to the previous dataset (1997). For the GM phase the retracked dataset was used. The different standards used in the old and new data set are shown in the box "data standards". After a quality check of the data, first the impact of this retracking is shown for significant wave high (SWH). Then, performances of the sea surface height (SSH) updated dataset at crossovers is shown and compared to the old dataset.

GEOSAT Mission :

Launched in March 1985 and ended its mission in January 1990 due to degradation of altimeter output power.¹

1-Geodetic Mission (GM): from March 1985 to September 1986 (18 months).

Main objective: to obtain a density sample map of marine geoid.

2-Exact Repeat Mission (ERM): from November 1986 to January 1990

Main objective: physical oceanography, study of fronts, wave, winds and ice.

Data standards:

*: CLS updated fields.

| Fields | RADS updated data-set | Old data-set (1997) |
|------------------------------|---|---|
| Orbit: | STD0905 Orbit ⁴⁾ (based on EIGEN_GL04S) | 1997- JGM-3 GDR Orbit |
| Ocean tide: | GOT 4v8 | GOT99* or CSR-3(1995) |
| Load tide: | GOT 4v8 | GOT99* or CSR-3(1995) |
| MSS: | CNES / CLS 2011 | CLS 2001* or MSS 1995 |
| Wet tropospheric correction: | ECMWF ERA-int. model | NCEP/NCAR model (1996) |
| Dry tropospheric correction: | ECMWF ERA-int. model | NCEP/NCAR model (1996) |
| Sea State Bias | Hybrid SSB | SSB 3 parameters |
| Ionospheric correction: | Ionospheric correction NIC-09 | Ionospheric correction IRI 95 (1997) |

The table shows the standards used for the study. Some of the 1997 corrections were already previously updated with some slightly more recent standards. Among several standards available for the same correction in the RADS database, the ones listed in the table were chosen.

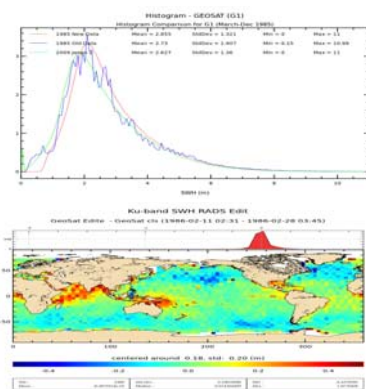
For the GM phase the retracked data (notably the range fib1) were used².

Retracking impact on SWH:

During the retracking of the GM phase, several parameters were derived from the waveforms³. Hereafter we compare Significant Wave Height (SWH) before and after retracking.

As retracked SWH (red curve) is available with a mm resolution its histogram is much smoother than the old SWH (available only with a cm resolution, blue curve)

Furthermore especially waves in low wave regions have higher values for the retracked data set.



SLA comparison:

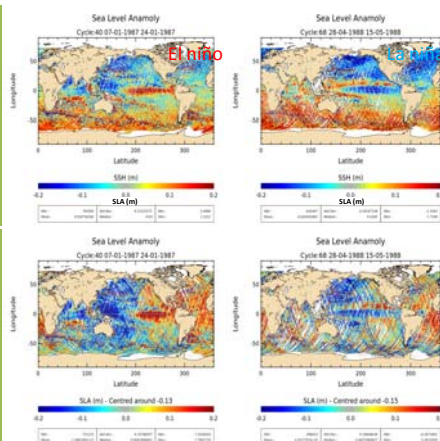
The strong East-West bias visible on sea level maps from 1997 dataset are no longer present in the new dataset.

Climatic phenomena like El Niño and la Niña are now clearly observable in new dataset.

Nevertheless, there are still geographical correlated errors in the dataset (North / South bias).

New data set

Old data set

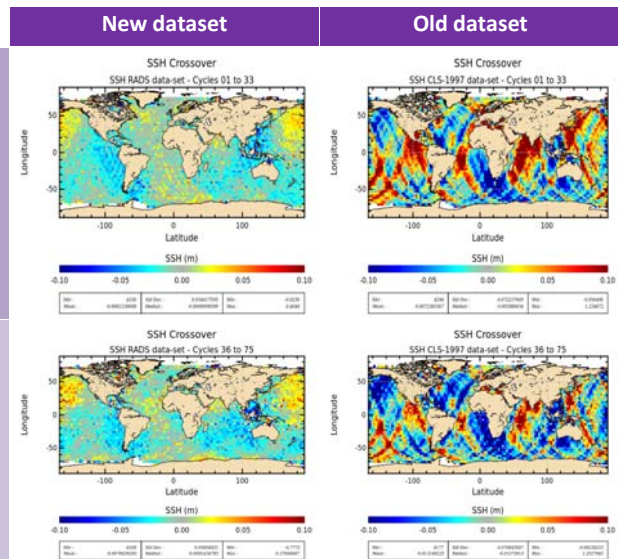


Comparison of SSH performances at crossovers:

SSH differences at crossover points are compared for ΔT (between ascending/descending tracks) <10 days. Outside areas of high oceanic variability the ocean does not change much over this period and SSH differences between ascending and descending passes should be ideally close to zero. SSH crossover maps of the old dataset show strong geographically correlated orbit errors.

GM Phase
(March 1985
to Sept. 1986)

ERM Phase
(Oct. 1986 to
Sept 1988)



Using the new dataset which contains the GSFC orbit (based on EIGEN_GL04S) strongly reduces these biases and show an improved homogeneity between ascending and descending passes.

Long term monitoring:

Cycle per cycle monitoring of mean and standard-deviation of SSH differences at crossovers also show strongly improved performances of the new data set. Standard-deviation is reduced from 12cm (old dataset) to 8.9cm.

Note that statistics after September 1988 are not shown due to reduced data coverage.

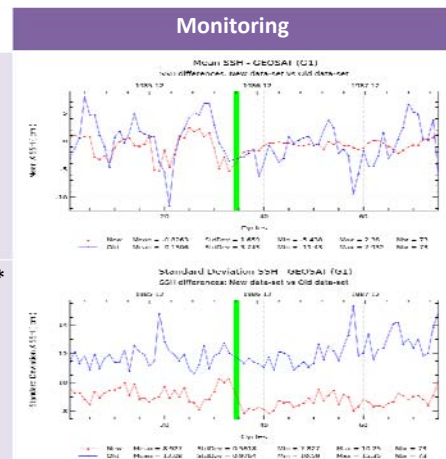
Mean: *
(until degradation)

! old data
! new data

Standard - *
deviation:
(until degradation)

! old data
! new data

*: monitoring to cycle 75 (Septembre 1988)



Summary & Conclusions:

The Updated GEOSAT dataset shows a strong improvement (especially thanks to GSFC orbit standard) at crossovers. SSH differences between ascending and descending passes are now much more consistent.

Climatic phenomena such as El Niño and La Niña are now clearly identifiable on Sea Level Anomaly maps.

Nevertheless, a hemispheric North / South effect is present in the new dataset. It is probably related to orbit errors.

References:
1) Nasa geosat: http://ibis.grdl.noaa.gov/sat/cdr/geosat_handbook/docs/chap_1.htm
2) Retracking method: David F. Sandwell and Walter H.F. Smith. Retracking ers-1 altimeter waveforms for optical gravity field recovery. *Geophys.J.Int.*, (163):79-89, 2005
3) John Lillibrige, Walter H.F. Smith, David Sanwell, Remko Scharroo, Frank G. Lemoineand, and Nikita P. Zelensky. + 20 years of improvements to GEOSAT Altimetry, March 2008
4) N. Zelensky et al. Precise orbit determination for Geosat and Geosat Follow-On. Poster OSTST 2010, Lisbon, Portugal. Available at <http://www.aviso.oceanobs.com/fileadmin/documents/OSTST/2010/Zelensky.pdf>